Universidade de Aveiro Departamento de Física
2009

Carina de Lurdes Bastos Lopes

Impactos da subida do nível médio do mar na Ria de Aveiro no séc. XXI

Impacts of sea level rise in Ria de Aveiro lagoon during 21st century

Universidade de Aveiro Departamento de Física
2009

Carina de Lurdes Bastos Lopes

Impactos da subida do nível médio do mar na Ria de Aveiro no séc. XXI

Impacts of sea level rise in Ria de Aveiro lagoon during 21st century

Dissertação apresentada à Universidade de Aveiro para cumprimento dos requisitos necessários à obtenção do grau de Mestre em Meteorologia e Oceanografia Física, realizada sob a orientação científica do Doutor Paulo Manuel Cruz Alves da Silva, Professor Auxiliar do Departamento de Física da Universidade de Aveiro e do Doutor João Miguel Sequeira Silva Dias, Professor Auxiliar do Departamento de Física da Universidade de Aveiro.

Este trabalho foi desenvolvido no âmbito do projecto G-Cast (GRID/GRI/81733/2006) com o apoio financeiro da Fundação para a Ciência e Tecnologia – FCT.

o júri

presidente

Prof. Doutor Alfredo Moreira Caseiro Rocha
Professor Associado com Agregação do Departamento de Física da Universidade de Aveiro

Prof. Doutor Paulo Manuel Cruz Alves da Silva
Professor Auxiliar do Departamento de Física da Universidade de Aveiro

Prof. Doutor João Miguel Sequeira Silva Dias
Professor Auxiliar do Departamento de Física da Universidade de Aveiro

Prof. Doutor Rui Pires de Matos Taborda
Professor Auxiliar do Departamento de Geologia da Faculdade de Ciências da Universidade de Lisboa

acknowledgements

The research in this thesis would have taken far longer to complete without the encouragement from many others. It is a delight to acknowledge those who have supported me over the last year.

First I wish to thanks my family, specially my parents, my boyfriend and my daughter for their love and encouragement.

I am especially thankful to my colleagues Sandra, Ana and Magda for their exceptional support. Sandra has been always available to answer my questions, and pointed me in the right direction.

I would like to thank my supervisors for their guidance, help and advice. This work will not be the same without their counsels and suggestions.

I want acknowledge to Prof. Alfredo Rocha for his advice and guidance in the elaboration of sea level rise scenarios. I have not doubt that without his help this work will be poorer.

I want to thank to Anabela Oliveira, André Fortunato and Xavier Bertin from LNEC not only for the technical support with MORSYS2D but also for the suggestions during G-Cast meeting.

I acknowledge the modeling groups, the Program for Climate Model Diagnosis and Intercomparison (PCMDI) and the WCRP's Working Group on Coupled Modelling (WGCM) for their roles in making available the WCRP CMIP3 multi-model dataset. Support of this dataset is provided by the Office of Science, U.S. Department of Energy.

palavras-chave

Ria de Aveiro; alterações climáticas; aumento do nível do mar local; modelo morfodinâmico; transporte de sedimentos; prisma de maré

resumo

A Ria de Aveiro é uma laguna mesotidal pouco profunda localizada na costa Noroeste de Portugal. Vários estudos mostram que a sua origem e evolução morfológica está associada a oscilações climáticas que induziram flutuações locais no nível médio do mar. Uma recente análise de dados registados no marégrafo da Ria de Aveiro revelou um aumento do nível médio do mar à entrada da laguna.

Este trabalho tem como objectivo avaliar o impacto do aumento do nível médio do mar na hidrodinâmica da laguna e na morfodinâmica da sua embocadura durante o século XXI. Para avaliar esse impacto foi aplicado o modelo morfodinâmico MORSYS2D previamente implementado e calibrado para a Ria de Aveiro.

Foram feitas projecções locais do aumento do nível médio do mar para o período 2071-2100 relativamente ao período de referência1980-1999, para diferentes cenários SRES desenvolvidos pelo IPCC. As projecções revelaram um aumento do nível médio do mar entre 0.25 m para o cenário B1 e 0.34 m para o cenário A2.

Os resultados dessas projecções foram utilizados para forçar o modelo morfodinâmico MORSYS2D. Os resultados obtidos a partir do MORSYS2D permitiram calcular o balanço sedimentar e o prisma de maré em algumas secções da laguna, identificando regiões com tendência erosiva e outras com tendência para sedimentação. Em geral, o transporte residual de sedimentos na laguna faz-se em direcção ao mar, no entanto os sedimentos tendem a ficar depositados na laguna, devido ao fraco transporte de sedimentos existente na embocadura. Com o aumento do nível médio do mar verifica-se uma tendência para o aumento da acreção na laguna face à situação actual.

Esperam-se também mudanças na hidrodinâmica da laguna resultantes do aumento do nível médio do mar. Estima-se um aumento do prisma de maré à entrada da laguna de cerca de 28% para o cenário A2 e 22% para o cenário B1, em relação ao prisma de maré calculado para o presente nível médio do mar.

keywords

Ria de Aveiro; climate change; local sea level rise; morphodynamic model; transport of sediments; tidal prism

abstract

Ria de Aveiro is a shallow mesotidal lagoon located in the northwest coast of Portugal. Various studies show that its origin and morphological evolution are associated with climate variability that induces local fluctuations in mean sea level. Analysis of recent tide gauges recorded data of Ria de Aveiro revealed a mean sea level increase on the mouth of this lagoon.

The purpose of this study is to evaluate the impact of mean sea level rise in the lagoon hydrodynamics and inlet morphodynamics during the 21st century. To assert this impact, the morphodynamic model MORSYS2D, previously implemented and calibrated for Ria de Aveiro lagoon, was applied in this study.

Projections of local sea level rise for the period 2071-2100 relative to 1980-1999, for different SRES scenarios developed by IPCC were made. The projections revealed an increase in the mean sea level between 0.25 m under scenario B1 and 0.34 m under scenario A2.

These sea level rise projections were used to force the MORSYS2D model. From the MORSYS2D results were compute the sediment balance and the tidal prism at some lagoon sections and detected regions with eroding and accreting trends. In general the transport of sediments in the lagoon is seaward, however the sediments tend deposite inside the lagoon, due to the weak sediment transport at the mouth. The increase in sea level suggests an increase of the accretion of sediments in the lagoon when compared with actual conditions.

Changes in the hydrodynamics of the lagoon are expected, as a result of the increase in mean sea level. In this study it is only analysed the tidal prism evolution. It is estimated an increase in tidal prism at the mouth of about 28% for scenario A2, and 22% for scenario B1, relative to tidal prism for the present mean sea level.

Contents

1 – Introduction 1

1.1 – Motivation and objectives 1

1.2 – State of the art 2

1.3 – Structure of the work 4

2 – Sea level rise scenarios 5

2.1 – GISS-ER model 6

2.2 – Local sea level rise projections 8

2.3 – Discussion 11

3 –Ria de Aveiro: lagoon hydrodynamics and inlet morphodynamics 15

3.1 – Study area 15

3.2 – Ria de Aveiro origin and morphological evolution 16

3.3 – Morphodynamic model 18

3.4 – Characterization of lagoon hydrodynamics and inlet morphodynamics 20

3.4.1 – Present mean sea level 20

3.4.2 – Changes induced by a mean sea level rise 29

3.5 – Limitations of morphodynamic predictions 37

4 – Conclusions 39

5 – References 43

List of Figures

2.1 - Factors that contribute to sea level change..... 5

2.2 - Variation in sea level (m) during 2071-2100 relative to 1980-1999 period, for the SRES scenario A2, in the North Atlantic. 9

2.3 - Sea level rise evolution (m) relative to 1980-1999, for the SRES scenarios A2, A1B and B1, at each of the eight points considered. 9

3.1 – Satellite image from Ria de Aveiro lagoon (extracted from Google Earth)..... 15

3.2 - Ria de Aveiro development. A – When it was a bay (10^{th} century); B – The sandbank growing southward (15^{th} century); C – Actual configuration of Ria de Aveiro (19^{th} century). (Extracted from Dias et al., 1994) 17

3.3 - Flowchart of MORSYS2D procedure every morphodynamic time step. 18

3.4 - Horizontal grid for Ria de Aveiro lagoon. The orange represents the ELCIRC grid and the black the SAND2D grid. 19

3.5 - Ria de Aveiro lagoon: a) Cross-sections location where tidal prism was evaluated (A to E); b) Cross-sections location where transport of sediments was computed (1 to 6) and regions where sedimentation rates were computed (I to IV). The point P represents a generic point where sea surface height and the sediment flux were analysed. 21

3.6 - Temporal evolution of sea surface height (left) and sediment flux (right), at a generic point in the inlet. 22

3.7 - Residual sediment flux (m^2/s) field at Ria de Aveiro inlet for 2001 bathymetry survey. 24

3.8 - Depth difference field between bathymetries of June of 2001 and September of 2005, a) predicted and b) observed. 25

3.9 – Relative error (%) between bathymetries. a) Er_1 and b) Er_2. 27

3.10 - Difference field between Er_2 and Er_1. 27

3.11 – Residual sediment transport trend into cross-sections, for present mean sea level and for the sea level rise scenarios A2 and B1. 32

3.12 – Residual sediment transport trend outward cross-sections, for present mean sea level and for the sea level rise scenarios A2 and B1. 32

3.13 – Residual net sediment transport trend, for present mean sea level and for the sea level scenarios A2 and B1. 33

3.14 - Residual sediment flux fields for SLR scenarios: a) A2 and b) B1. 34

3.15 - Difference fields between residual sediment fluxes for present mean sea level and SLR scenarios: a) A2 and b) B1. 35

3.16 - Sedimentation rates computed from predicted bathymetries for present mean sea level and for SLR scenarios A2 and B1. 36

3.17 - Tidal prism in each cross-section for spring tide (left) and neap tide (right) conditions. 36

List of Tables

2.1 - Summary characteristics of the SRES scenarios A2, A1B and B1 (adapted from Carter et al., 2007). 8

2.2 - Mean ($\bar{u}$) and standard deviation (σ) of sea level change, relative to the 1980-1999 period, for the 20C3M simulation, and for the 2071-2100 period at the grid points presented in Figure 2.1. 10

2.3 - Rate of sea level change due to GIA at some locations in Portugal. 11

2.4 - Sea level rise projections for 2071-2100 related to 1980-1999 in Portugal. 11

2.5 - Global sea level rise projections for 2090-2099 in relation to 1980-1999. 12

3.1 - Sediment transport (m^3/day) through cross-sections at extreme spring tide, neap tide and residual conditions. 23

3.2 - Sedimentation rate (m^3/day) between cross-sections from 2001 to 2005 and from 2001 to 2007 both observed and predicted. 24

3.3 - Tidal prism (m^3) at spring tide and neap tide conditions both from observed and predicted bathymetries 28

3.4 - Sediment transport (m^3/day) through cross-sections at extreme spring tide, neap tide and residual conditions, for scenario A2. 30

3.5 – Sediment transport (m^3/day) through cross-sections at extreme spring tide, neap tide and residual conditions, for scenario B1. 31

3.6– Sedimentation rate (m^3/day) between cross-sections between 2094 and 2100 for SLR scenarios A2 and B1. 35

3.7– Projected tidal prisms ($\times 10^6$ m^3) at neap tide and spring tide conditions under SLR scenarios A2 and B1. 36

1 – Introduction

1.1 – Motivation and objectives

Coastal regions are dynamic interface zones where land, water and atmosphere interact in a fragile balance that is constantly being altered by natural and human influence. Natural pressures includes storms, wind, tides, waves, sea level and runoff while anthropogenic pressures includes all human activities such as fisheries, coastal agriculture, tourism and coastal builds. Generally, coastal areas are extremely productive and accessible to people. Therefore these areas are densely populated, intensifying the anthropogenic pressures. The natural pressures are also being intensified in result of the climate change. The dominant factor in the radiative forcing of climate in the industrial era is the increasing concentration of various greenhouse gases in the atmosphere. Several of the major greenhouse gases occur naturally, but increases in their atmospheric concentrations over the last 250 years are due largely to human activities (Solomon et al., 2007). Global mean sea level has been rising in the last century and it is expected that sea level continues to rise in this century as result of ocean thermal expansion and melting of mountain glaciers, ice caps and ice sheets (Nicholls et al., 2007). The impacts of sea level rise (SLR) on coastal areas have been studied by many scientists in the world, and the generalized physical consequences are inundation on coastal areas, landward intrusion of salt water in estuaries and aquifers and coastal erosion.

Ria de Aveiro lagoon is an example of one coastal ecosystem very dynamic and extremely rich in fauna and flora. Along the years people was fixed around the lagoon and have explored its resources. The evolution of the lagoon indicates that human action has been the major factor controlling the lagoon (Silva and Duck, 2001). The most remarkable man work was the built of an artificial inlet in 1808, which have changed deeply the hydrodynamics of the lagoon. Analysis of recent tide gauges data (1976-2003) revealed a mean sea level increase at the lagoon mouth at the rate of 1.15±0.68 mm/year (Araújo, 2005), a rate that would have a significant impact in the lagoon hydrodynamics and morphodynamics.

The primary aim of this study is to characterize the hydrodynamics of the lagoon and the morphodynamics at the inlet, as well as to estimate the hydrodynamic and morphodynamic changes induced by sea level rise as a result of climate change of anthropogenic nature. With this purpose, scenarios of local SLR relative to present (reference period) mean sea level were determined in order to force the morphodynamic model system MORSYS2D previously implemented and calibrated for Ria de Aveiro lagoon by Oliveira et al. (2006). The reference period was 1980-1999 and the projected scenarios are referred to 2071-2100 period.

1.2 – State of the art

SLR is an important aspect of climate change because of its impacts on coastal areas. In general the physical effects of SLR on coastal areas are coastal inundation, erosion, salt water intrusion and ecosystems loss (Nicholls et al., 2007). Some studies have been performed to evaluate the impact of SLR along the Portuguese coast (Ferreira et al., 2008 and Andrade et al., 2006) which showed that low-lying areas like estuaries, coastal lagoons and wetlands are considered areas of high vulnerability to SLR. Silva and Duck (2001) have performed a study about the morphological evolution of Ria de Aveiro, and based on past trends they have identify some processes expected for future: an increase in salinity; reduction of area covered by sea plants; erosion of mud flats, salt marsh and salt pans; and redistribution of sediments between compartments of the system and the ocean. They have also estimated that an increase of 0.1 m in mean sea level produces an increase of 22% in the tidal prism.

In a recent work (Araújo, 2005) were analysed the sea level changes in the lagoon through the comparison between sea level elevations from two different surveys (1987/88 and 2002/03). A generalized increase in the amplitude and decrease in the phase was found, for most of the harmonic constituents. Changes in the tidal characteristics of the lagoon have been associated to changes in tidal prism at the inlet, as a result of the intensive engineering works. Araújo et al. (2008) have investigated how changes of the inlet and other lagoon factors may have influenced the tidal dynamics of the lagoon. They have found that the tidal changes are affected predominantly by changes in the depth of the inlet channel. A raise in the mean depth induces an increase in the amplitude and a decrease in the phase of M_2 constituent (the major constituent in the lagoon) overall the lagoon.

However, an increase in the total area of the lagoon (as a result of land reclamation, dredging, erosion...) leads to a decrease in the amplitude and an increase in the phase of M_2 constituent.

More recently, Coelho et al. (2009) have studied the potential impacts of climate change on the northwest coast of Portugal and shown that the sand-spit disruption is expected, as well as an ultimate linkage between the sea and the lagoon of Aveiro.

To evaluate the impacts of SLR on coastal areas it is essential to estimate the local SLR, considering that the rise in sea level is non-uniform in space (Nicholls et al., 2007). Dias and Taborda (1988) predicted a SLR for Portugal between 0.14 m and 0.57 m by the year 2100, based on extrapolation of simple fits to observed data from tide gauges of Cascais (105 years) and Lagos (78 years). More recently, Antunes and Taborda (2009) have estimated a SLR between 0.19 and 0.75 m in 2100, based on the same method, but considering the period 1977-2008 of Cascais tide gauges, which have registered a more emphasized SLR rate in this period. In this work a different method was used to estimate SLR for 2100, the climate modelling. The projections obtained will be compared with those estimates based on extrapolation of fitted data.

Many studies have been performed in order to evaluate the hydrodynamics of Ria de Aveiro lagoon. Dias (2001) has concluded that the tide is the main forcing controlling the lagoon hydrodynamics and has estimated the tidal prism at the inlet for a maximum spring tide of 3.2 m and a minimum neap tide of 0.6 m (136.7×10^6 m^3 and 34.9×10^6 m^3, respectively). These values are higher than those estimated more recently by Picado (2008), 86.3×10^6 m^3 and 31.0×10^6 m^3 for a spring tide of 3.0 m and a neap tide of 0.7 m, respectively. Picado (2008) also showed that the tidal prism at the inlet tends to increase with the destruction of the salt pans walls. This increase was quantified and was found to be about 2.5% for extreme destruction of the salt pans walls.

A hydrological characterization performed by Dias et al. (2000) showed that the lagoon can be generally considered vertically homogeneous, but in exceptional situations of very strong fresh water flows the lagoon presents some vertical stratification. Recently, Vaz et al. (2008) have demonstrated that during the wet season the Vouga river flow induces stratification from the Espinheiro channel to the lagoon mouth.

Extreme conditions of strong wind may also influence the circulation in the lagoon during short periods, mostly in shallow areas and wide channels (Dias, 2001).

The dynamics of sediments is essentially determined by tidal forcing. Lopes and Dias (2007) performed a study about residual circulation and sediment distribution in the Ria de Aveiro lagoon. They have concluded that the residual circulation is determined by the asymmetries between flood and ebb regimes. As the lagoon is ebb-dominant there is a trend to export sediments to the ocean. They have also concluded that the magnitude of residual currents generated by wind and river runoff is one or two orders of magnitude lower than the residual tidal currents.

The morphodymanics of the lagoon was not so deeply studied as its hydrodynamics. Indeed, the bathymetric variations were analysed only in the inlet evolving zone by Plecha et al. (2007, 2009). These studies focuses in the bathymetric changes occurred from 1987/88 (after the prolongation of the northern breakwater) until 2005. They have concluded that the physical changes imposed by the prolongation of breakwater in conjunction with the regular channel dredging, leaded to a deepening of the inlet channel. The largest depth increase occurred between the head of the southern breakwater and the northern breakwater and close to the tidal gauge. They have also identified accretion trends at Meia Laranja beach, at several zones in the main channel and at the head of the northern jetty. They have also concluded that the deeper areas around the inlet are migrating offshore, deepening at the left side of the channel and accreting at the left side. In this work, sedimentation rates were computed in order to quantify the erosion and the deposition at some regions around the inlet.

1.3 – Structure of the work

The structure of this work is constituted by more three chapters. Chapter 2 presents the projections of SLR for the Aveiro region. Formulations of SLR scenarios (2071-2100 period relative to 1980-1999 period) were made processing data of an Atmosphere-Ocean General Circulation Model (AOGCM), the GISS-ER model (Russel et al., 1995, 2000).

In Chapter 3 a description of Ria de Aveiro lagoon is presented and the model MORSYS2D used to characterize the inlet morphodynamics is described. Furthermore, the results of simulations with MORSYS2D model are presented both for present mean sea level and for SLR projected scenarios.

The work closes with Chapter 4 where the main conclusions of this study are presented and suggestions for the future research are formulated as a way to improve the present results.

2 – Sea level rise scenarios

Sea level may be modified by several factors at different characteristic temporal and spatial scales. A sea level change may occur from seconds to centuries. Figure 2.1 summarizes the factors that may contribute to sea level change according to Chao et al. (2002.) The short term oscillations as generated by wind or tides don't have influence on mean sea level. The mean sea level is altered by long term oscillations that can be caused by volume change (thermal expansion and long term dynamic change), mass exchange (melting of mountain glaciers and ice caps and changes in Greenland and Antarctic ice sheets) and land subsidence (vertical movements in the solid earth related to tectonics and isostatic adjustment). The thermal expansion is the reply of the ocean to global atmospheric temperature rise and the long term dynamic change result of density gradients: this includes meteorological oscillations such as ENSO (El Niño-Southern Oscillation) and NAO (North Atlantic Oscillation), which influence deep thermohaline circulations.

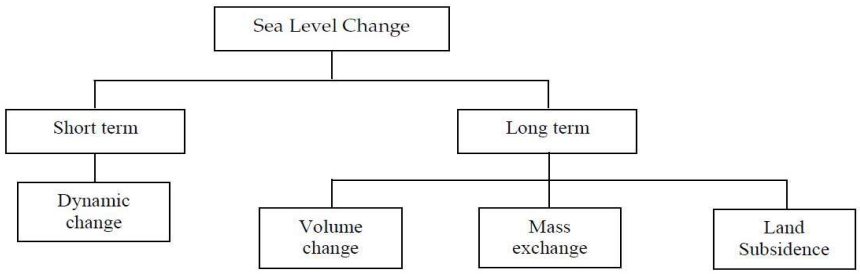

Figure 2.1 - Factors that contribute to sea level change.

The major contribution to global mean SLR which is expected during 21st century is the thermal expansion. This contribution was estimated as about 70% by Meehl et al., (2007a). The exchange of water between ocean and others reservoirs has also a significant contribution to global mean sea level, about 30% (Meehl et al., 2007a). It is also known that changes in the mean sea level are non-uniform in space. There are regions where the increase of sea level is several times higher than the overall average sea level change, while in other locations sea level change is lower than their global average (Meehl et al., 2007a). Then a good local projection of local SLR has to attend to local factors such as long term dynamic change (their global mean is close to zero) and land subsidence.

In this way, instead of using the projected global average sea level publicised in the last IPCC (Intergovernmental Panel on Climate Change) report, simulated by a set of seventeen AOGCMs, the output of GISS-ER model (Russel et al., 1995, 2000) was used to estimate the spatial distribution of SLR in the Portuguese coast. The GISS-ER model was chosen because within the seventeen AOGCMs it is the only one that outputs a variable that in every grid point accounts for the change in sea level due to volume change and mass exchange. In the other models these effects must be added separately (Katsman et al., 2007).

2.1 – GISS-ER model

The GISS-ER model is a coupled atmosphere-ocean model developed at Goddard Institute for Space Studies (GISS) by Russell et al. (1995). It has a Cartesian grid with resolution of 4º of latitude by 5º of longitude. The atmospheric model has twenty layers in the vertical (ten sigma levels since surface to 150 hPa, and other ten pressure levels since 150 hPa to the model top at 0.1 hPa), while the oceanic model has thirteen vertical *z* levels (12, 18, 27, 40.5, 61, 91, 137, 205, 308, 461, 692, 1038 and 1557 meters). The resolution for heat, water vapour, and salt is thinner than the grid resolution because those quantities have both means and prognostic directional gradients inside each grid box. This information is used in the advection by the linear upstream scheme, and atmospheric condensation and ocean vertical mixing are performed on 2º by 2.5º horizontal resolution.

The atmospheric model is composed by models that solve different physical parameterizations (e.g. radiation, cloud processes, atmospheric turbulence, surface fluxes and land surface processes).

The radiation model calculates explicitly multiple scattering for short wave (SW) radiation and makes explicit integrations over both SW and long wave (LW) spectral regions. The SW radiation is absorbed by H_2O, CO_2, O_3, O_2 and NO_2. The LW radiation is absorbed by H_2O, CO_2, O_3, CH_4, N_2O CFC-11 and CFC-12.

The cumulus and stratiform parameterization is estimated by a model that uses the mass flux approach (it is assumed within some area taken to be the grid point of a numerical model, that a fraction is covered by cloud) to cumulus parameterization. Convection can be triggered at any model level when an air parcel lifted one model layer, saturates and becomes buoyant. Cumulus are produced for parcels that ascend more than one model

level at which an equal mixture of cloud and environmental air is negatively buoyant. Stratiform cloud water is treated prognostically, with cloud formation based on moisture convergence. The scheme includes simple representations of microphysical sources and skins of cloud water (e.g. auto-conversion, evaporation...).

The atmospheric turbulence is calculated in the whole column, but the model has a formulation for planetary boundary layer (PBL) processes and a different formulation for the atmosphere above the PBL.

The surface fluxes are calculated using a model that is embedded between the surface and the midpoint of the first resolved model layer.

The land surface model incorporates a model for snow and hydrology and a model for vegetation. These models try to solve some feedbacks between the atmosphere and surface.

The ocean model solves the processes in the ocean mixing boundary layer near the surface under a variety of surface forcing conditions, and mixing in the ocean interior due to internal waves, shear instability and diffusion. For that the model uses de k profile parameterization scheme (Large et al., 1994). The model also includes bottom friction.

Given the relatively coarse horizontal resolution in the ocean model, it was necessary to incorporate straits in the model in order to allow the passage of water through grid boxes which would otherwise be classified as all land. The mass of water is non-divergent (the mass flow is accelerated only by pressure gradient force). Twelve straits are included in the model.

The ocean model has a free surface, allowing water mass divergence and interaction with the atmosphere. Continental river flow from the atmospheric model is added to the ocean with proper location and timing.

The physics time step for both models is 30 minutes, allowing synchronous coupling every 30 minutes.

Climate GISS-ER model output from simulations of the past (pre-industrial run), present (20C3M run) and future climate (different scenarios runs) have been made available to the scientific community by the World Climate Research Programme's (WCRP's) Coupled Model Intercomparison Project phase 3 (CMIP3) multi-model dataset (Meehl et al., 2007b). The 20C3M run starts at 1880 and ends at 2003. The output of 20C3M run is used to initialize the future climate runs starting at 2004 and finishing at 2100. The future climate was simulated by the model imposing different emission scenarios of greenhouse

gas developed by IPCC. In this work three SRES (Special Report on Emission Scenarios) scenarios are considered A2, A1B and B1. Detailed information about SRES scenarios is available at http://sres.ciesin.org/.The emission scenarios are quantified trough the CO_2 equivalent concentration (is the amount of CO_2 concentration that would cause the same time-integrated radiative forcing as a given type and concentration of greenhouse gas) based on a range of possible behaviours of society, economy and technology (Table 2.1).

Table 2.1 - Summary characteristics of the SRES scenarios A2, A1B and B1 (adapted from Carter et al., 2007).

	Development			**Surrogate stabilisation scenario**
	Population	Economy	Technology	
A2	Continuously increasing	Moderate growth	Slowest development	Does not stabilise
A1B	2050 peak then decline	Accentuated growth	Balanced across all sources	750 ppm
B1	2050 peak then decline	Not so accentuated than A1B	Clean and resource-efficient	550 ppm

2.2 – Local sea level rise projections

The GISS-ER model calculates, for every grid point, the sea surface height above the geoid due to volume fluctuations and to the exchange of water between ocean and other reservoirs.

With sea surface height data given by GISS-ER model, the change in sea level relative to the actual (reference) mean sea level simulated by GISS-ER model was computed for the 21st century (2071-2100 period), for each considered scenario. The reference was considered to be the mean for the 1980 to 1999 period. Figure 2.2 shows sea level change, for the North Atlantic region, under scenario SRES A2, revealing a rise in sea level for the whole region. It shows very weak spatial variability of SLR near the Portuguese coast.

To minimize sampling problems associated with uncertainty of the model at small spatial scales, the behaviour of sea level change at eight points (represented in Figure 2.2) surrounding the region of interest was analysed. Figure 2.3 shows the evolution of

simulated sea level change at each point, during the present climate (the 20C3M curve represents the 1970-2003 period only at *P1*) and for each of the three scenarios, until 2100. From the analysis of this figure is confirmed the weak spatial variability among the points considered.

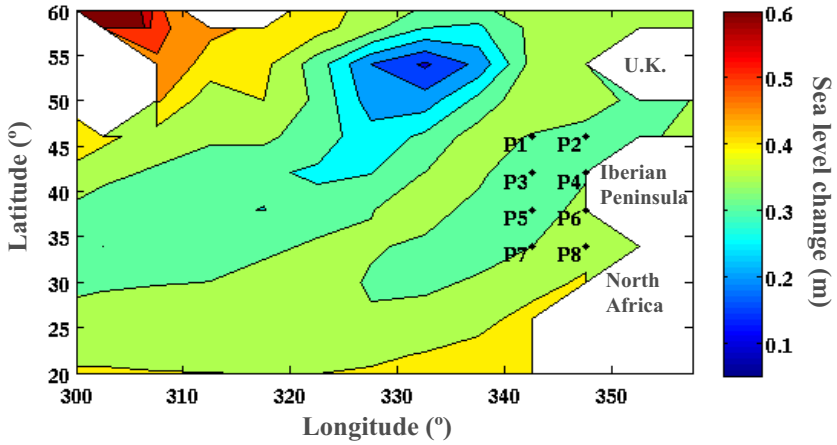

Figure 2.2 - Variation in sea level (m) during 2071-2100 relative to 1980-1999 period, for the SRES scenario A2, in the North Atlantic.

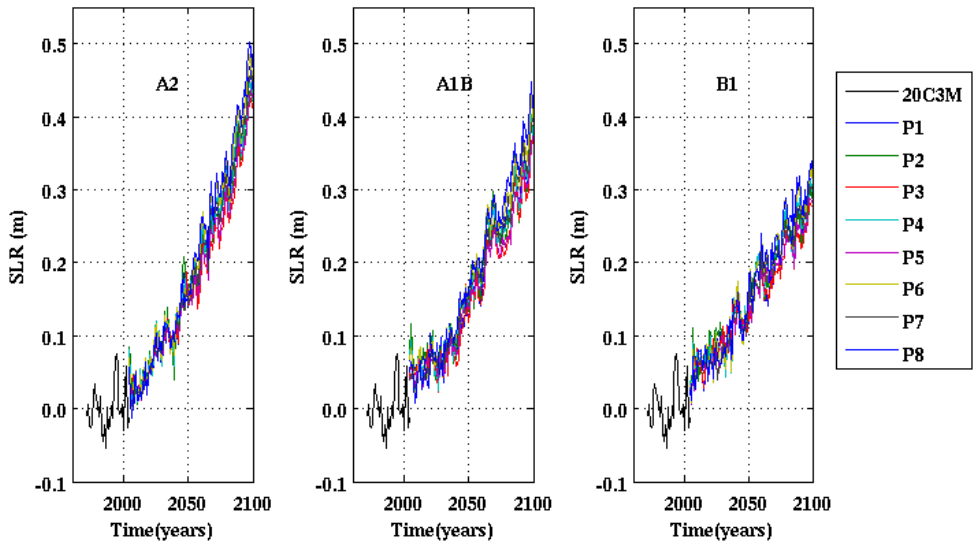

Figure 2.3 - Sea level rise evolution (m) relative to 1980-1999, for the SRES scenarios A2, A1B and B1, at each of the eight points considered.

Table 2.2 shows the mean and the standard deviation of sea level change, relative to the 1980-1999, for the 20C3M simulation, and for the 2071-2100 period. Again, it is evident the weak spatial variability among the considered points.

A t-student test revealed that the mean sea level at each of the eight points is significantly higher, at the 1% significance level, in the future climate when compared to the present climate. Also, an F-test showed that, in the future climate, the sea level variances at each of the eight points are not significantly (1% significance level) different, than those in the present climate.

Table 2.2 - Mean (ū) and standard deviation (σ) of sea level change, relative to the 1980-1999 period, for the 20C3M simulation, and for the 2071-2100 period at the grid points presented in Figure 2.1.

		20C3M	A2	A1B	B1
P1	ū (m)	2.6×10^{-3}	0.35	0.31	0.26
	σ ($\times10^{-2}$m)	3.1	2.1	2.7	2.0
P2	ū (m)	4.3×10^{-3}	0.34	0.29	0.25
	σ ($\times10^{-2}$m)	2.6	2.1	2.6	2.2
P3	ū (m)	2.1×10^{-3}	0.31	0.27	0.23
	σ ($\times10^{-2}$m)	2.6	2.0	2.1	1.6
P4	ū (m)	3.4×10^{-3}	0.34	0.29	0.25
	σ ($\times10^{-2}$m)	2.4	2.5	2.0	2.2
P5	ū (m)	2.3×10^{-3}	0.32	0.28	0.23
	σ ($\times10^{-2}$m)	2.3	2.0	1.7	1.4
P6	ū (m)	2.7×10^{-3}	0.36	0.32	0.27
	σ ($\times10^{-2}$m)	2.7	2.7	1.8	2.4
P7	ū (m)	1.2×10^{-3}	0.35	0.30	0.25
	σ ($\times10^{-2}$m)	2.3	1.9	1.5	1.5
P8	ū (m)	-3.0×10^{-4}	0.38	0.34	0.272
	σ ($\times10^{-2}$m)	2.7	2.4	1.7	2.3

The GISS-ER model data does not include the effect of land subsidence, so it was necessary to calculate, separately, this contribution to SLR in the Aveiro region. SLR due to land subsidence (SLR_{LS}) was accounted based on Peltier (2004), and using the rate of sea level change (R) due to Glacial Isostatic Adjustment (GIA) available at http://www.atmosp.physics.utoronto.ca/~peltier/datasets/psmsl/DRSL.PSMSL.ICE5G.VM2.L90.txt. Its contribution was evaluated by:

$$SLR_{LS} = R(T - T_B) \qquad (2.1)$$

where T is the year (ranging from 2004 to 2100) and T_B is the mean of reference period (1990). Table 2.3 presents values of the rate of sea level change due to GIA (R) at some locations in the Portuguese coast. As R is negative, the effect of land subsidence contributes to a decrease in sea level in Portugal. This contribution was evaluated, considering a mean value for R. The results obtained show that it represents a reduction of about 5% in sea level change. The contribution of land subsidence is weak when compared to the contributions of the other factors analysed before, so it was considered the exclusion of this effect in the projections presented here.

Table 2.3 - Rate of sea level change due to GIA at some locations in Portugal.

Location	*R* (mm/year)
Viana	-0.09
Leixões	-0.13
Aveiro	-0.14
Cascais	0.00
Lisboa	-0.04
Tróia	-0.06
Sines	-0.01

2.3 – Discussion

From the statistical analysis performed before it is concluded that there is weak spatial variability of sea level change in the region delimited by the eight points analysed, so it was considered that the change in sea level in the Portuguese coast is the mean of the values obtained in the points analysed. Table 2.4 presents the local SLR projections at the end of this century in relation to present sea level for the Portuguese coast. The worst scenario (A2) indicates an increase of 0.34 m and the most optimistic (B1) an increase of 0.25 m.

Table 2.4 - Sea level rise projections for 2071-2100 related to 1980-1999 in Portugal.

Scenario	SLR (m)
A2	0.34
A1B	0.30
B1	0.25

The local SLR projections presented here are within the range of global SLR projections presented in Table 2.5 and reported by Meehl et al. (2007a).

As the local projections reported here are based on climate modelling, there are many sources of related uncertainty. The first source of uncertainty comes from the estimated emission scenarios that force AOGCMs.

Table 2.5 - Global sea level rise projections for 2090-2099 in relation to 1980-1999.

Scenario	SLR (m)
A2	0.23 – 051
A1B	0.21 – 0.48
B1	0.18 – 0.38

The emission scenarios are quantified based on a range of possible behaviours of society, economy and technology. The translation of these behaviours into greenhouse gas emissions are extremely hard and uncertain (Morgan and Henrion, 1990). Other sources of uncertainty are related to some feedbacks in the carbon cycle and vegetation cycle that are not represented, or only very crudely represented in AOGCMs (Friedlingstein et al., 2006). There are also uncertainties related to AOGCMs physical processes. The AOGCMs are models and may not include relevant climate phenomenons because these may not be well understood. AOGCMs can also represent some physical processes and parameterizations in rather simple forms. Overall, every AOGCM has particular features that differ from the others models. So, if the output of another AOGCMs were considered, and a similar analysis performed the projection results would be certainly different. Gregory et al. (2001) revealed that there is not agreement about the geographic patterns of sea level rise at small scales, but at larger regional scales the patterns of sea level change simulated by those models are in agreement.

Anyhow, it is important to evaluate the local SLR, due to its impacts on coastal areas. Dias and Taborda (1988) predicted a SLR for Portugal between 0.14 m and 0.57 m by the year 2100, according to an empirical method based on the extrapolation of SLR rate obtained from observed data recorded by tide gauges of Cascais and Lagos. Using a similar method, Antunes and Taborda (2009) projected a rise of 0.47 m with a 95% confidence interval between 0.19 and 0.75 m in the year 2100 relative to 1990 mean sea level for Cascais. The values projected in the present work are based on climate modelling, which is physically

based and takes into account the nonlinear characteristic of the climate system and, moreover, the nonlinearity of the forcing (that may be different from the past forcing depending on the scenario considered). However, the results obtained by the empirical studies mentioned above are broadly similar to those reported here.

On the other way, the extrapolation of SLR rate at the Ria de Aveiro lagoon mouth published by Araújo (2005), 1.15±0.68 mm/year, indicates for 2100 an increase in mean sea level between 0.05 and 0.2 m. The inconsistency between these values and the projections reported here can be due to the fact that the tide gauge of Aveiro has a relatively short record (<50 years), which is unsuitable for long term mean sea level trend determination (Douglas, 1991).

3 –Ria de Aveiro: lagoon hydrodynamics and inlet morphodynamics

3.1 – Study area

Ria de Aveiro is a coastal lagoon located in the northwest coast of Portugal (Figure 3.1) and it is connected with the Atlantic Ocean by a single artificial inlet built in 1808. It is 45 km long and 10 km wide, and covers an area of 83 km^2 at high tide (spring tide), which is reduced to 66 km^2 at low tide (Dias and Lopes, 2006). It is characterized by narrow channels and by large areas of mud flats and salt marshes. Its main channels are Mira, S. Jacinto, Ílhavo and Espinheiro. Mira channel is 20 km long, and runs southward parallel to the coast. S. Jacinto channel is about 29 km long and runs northward parallel to the coast. Ílhavo and Espinheiro channels runs together eastward towards the town of Aveiro. After, Ílhavo channel turns southward and Espinheiro channel turns northeastward. Ílhavo channel is 15 km long and Espinheiro channel is 17 km long. Espinheiro channel receives the main input of fresh water in the lagoon by Vouga River. This input represents 2/3 of the total fresh water in the lagoon (Dias, 2001).

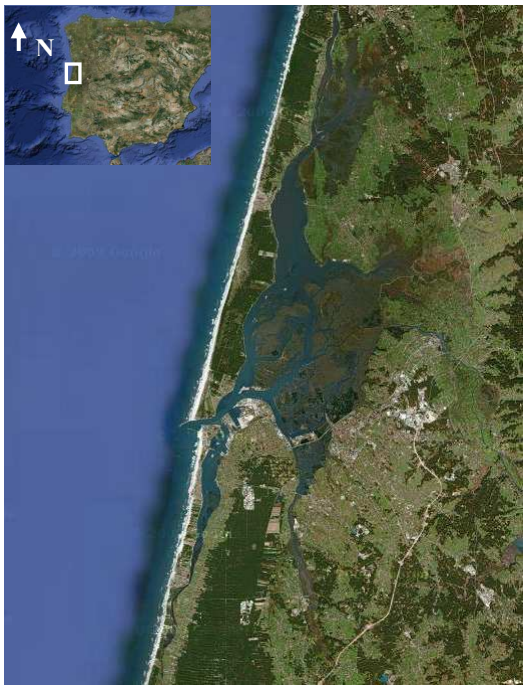

Figure 3.1 – Satellite image from Ria de Aveiro lagoon (extracted from Google Earth).

The hydrodynamics and morphodynamics of the lagoon are essentially dominated by tides, which are semidiurnal with a small diurnal pattern. The estimated tidal prism at the inlet varies from a maximum of 136.7×10^6 m^3 in spring tide to a minimum of 34.9×10^6 m^3 in neap tide while the freshwater input was estimated in 1.8×10^6 m^3 during a tidal cycle (Dias, 2001).

The lagoon can be considered vertically homogeneous during dry seasons. However, after important rainfall and consequent increase in the freshwater flows, the stratification becomes important near the mouth of the main rivers (Dias et al., 1999).

The contribution of wind and runoff to the residual circulation is one or two orders of magnitude lower than the tidal residual circulation. Thereby, the residual circulation is determined essentially by the asymmetries between the flood and ebb regimes. As the lagoon is ebb-dominant there is a trend to export sediments to the ocean (Lopes and Dias, 2007).

The lagoon adjacent coast is subjected to a highly energetic wave climate, typical of the west Portuguese coast, which leads to an average alongshore transport of about 1×10^6 m^3 (Larangeiro and Oliveira, 2003).

3.2 – Ria de Aveiro origin and morphological evolution

The origin and morphological evolution of Ria de Aveiro lagoon were associated with fluctuations in sea level caused by climatic oscillations. The little climatic optimum (X – XIV centuries) was characterized by high temperatures, and rise in mean sea level that would equal or was slightly higher than the current one, and the little ice age (XIV – XIX centuries) was characterized by low temperatures, and a decrease in mean sea level (Dias et al., 1994).

Figure 3.2 shows the evolution of Ria de Aveiro since it was a bay until the present, when it became a lagoon. Ria de Aveiro lagoon formation started about one thousand years ago in the little climatic optimum, forming a sandbank at Espinho, which grew southward. In the eighteenth century the sandy fillet arrived at Mira concluding the lagoon's formation (Dias et al., 1994).

During little ice age, the entire Portuguese coast showed a regressive behaviour, due to the discharge of river sediments. The transport of these sediments to the continental platform was favoured by the floods and by the lowering of sea level. This accretion had negative

impacts isolating the lagoon from the Atlantic Ocean (Dias et al., 1994). At that time the lagoon was river dominated and in wet periods the overall area was flooded by river water.

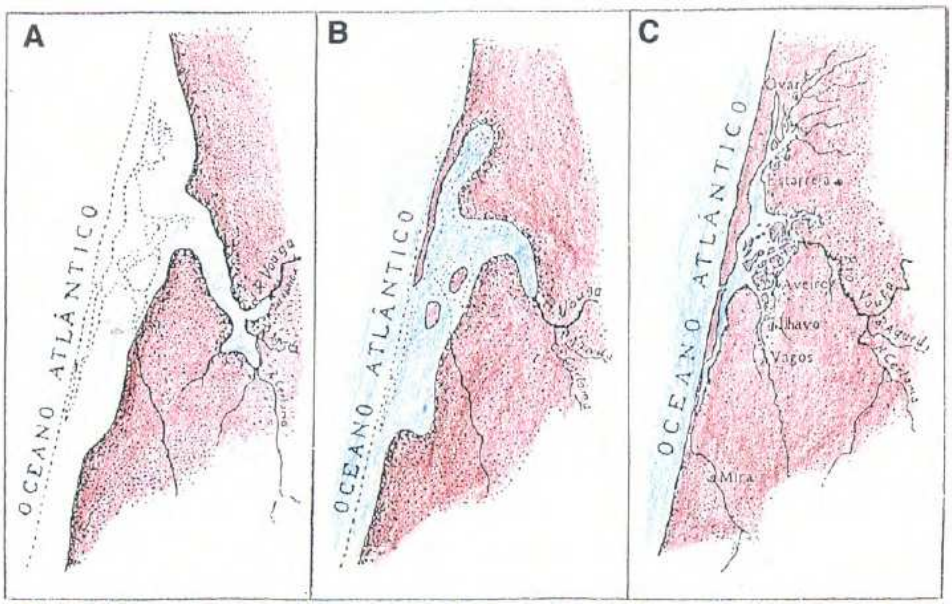

Figure 3.2 - Ria de Aveiro development. A – When it was a bay (10th century); B – The sandbank growing southward (15th century); C – Actual configuration of Ria de Aveiro (19th century) (Extracted from Dias et al., 1994).

In 1808 an artificial inlet was built, and the lagoon hydrodynamics was deeply altered, and became tidally dominated. This change was positive and brought many benefits to the population around the lagoon. However, this artificial inlet was many times partially destroyed by strong storms and to avoid this situation in 1936 was improved by the construction of a breakwater on the north embankment. In 1958 the south jetty was built and the north jetty was extended. Between 1983 and 1987 the north jetty was prolonged more 500 m finishing the heavy works around the inlet until the present. Since then the works at the inlet involving zone are essentially the dredging of main channels allowing the access to the Aveiro harbour and maintenance works in the breakwaters.

There is no doubt that the construction of the inlet brought many benefits to the region, however the extension of the jetties to the ocean, mainly the north jetty, had interrupted the littoral drift leading to serious problems of erosion southward the inlet. As can be observed on Figures 3.1 and 3.2 C), southward the inlet there is a sand dune that separates the ocean from the Mira channel. Recently this sand dune was overwashed by the sea during an episode of strong waves, evidencing the high vulnerability of this area to the advance of the sea.

3.3 – Morphodynamic model

The modelling system MORSYS2D simulates the non-cohesive sediment dynamics and bottom changes in estuaries, tidal inlets and coastal regions, driven by tides, waves, wind and river flows. The system integrates a hydrodynamic model (the user may choice between ELCIRC and ADCIRC), a wave model (the user may also choice between SWAN and REF/DIF1) and the sand transport and bottom update model SAND2D (Fortunato and Oliveira, 2004, 2007 and Bertin et al., 2009). The applications presented in this study use the modules ELCIRC and SAND2D (Figure 3.3). Although the wave forcing is very important in the morphodynamics of the inlets, it is despised in this study because it increases considerably the computational efforts.

The hydrodynamic model ELCIRC solves the shallow water equations (conservation of mass and momentum) using a finite volume technique for volume conservation and a natural treatment of wetting and drying. A semi-implicit time stepping algorithm and the Lagrangian treatment of the advective terms ensure stability at large time steps. The horizontal domain is discretized with a triangular mesh, and a single vertical layer reverting ELCIRC to a 2D depth-averaged model.

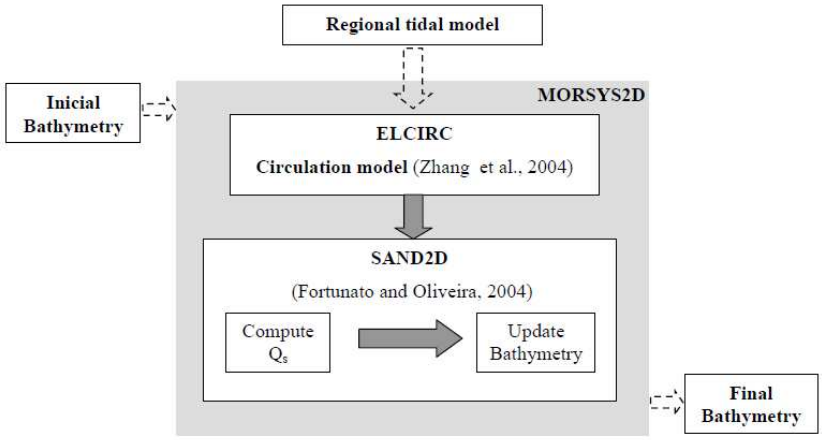

Figure 3.3 - Flowchart of MORSYS2D procedure every morphodynamic time step.

The SAND2D model simulates sand transport due to currents using one of several available semi-empirical formulae, and computes the resulting bed changes through the Exner equation:

$$\Delta h^i = \frac{1}{1-\lambda}\nabla Q_*^i \qquad (3.1)$$

where, Δh^i is the bottom variation over a time step, λ is the sediment porosity and Q_*^i is the sediment flux integrated over a time step.

The MORSYS2D was previously implemented and calibrated for Ria de Aveiro lagoon by Oliveira et al. (2006) in order to study the sediment dynamics at the inlet. The ELCIRC was implemented for the entire lagoon, but the SAND2D was implemented only for the inlet evolving area (Figure 3.4). Consequently the MORSYS2D solves the hydrodynamics for the entire lagoon, but updates the bathymetry only in SAND2D grid area. The ELCIRC grid has 18851 nodes and 29380 elements while the SAND2D grid has 1812 nodes and 3337 elements.

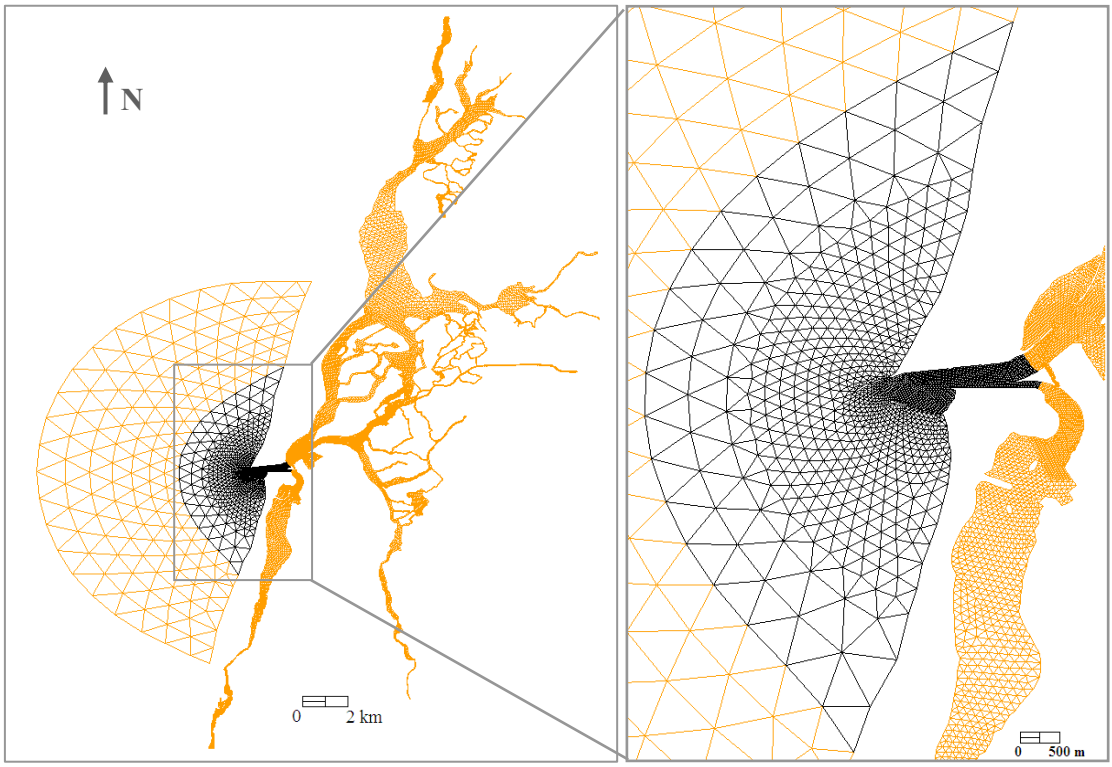

Figure 3.4 - Horizontal grid for Ria de Aveiro lagoon. The orange represents the ELCIRC grid and the black the SAND2D grid.

The simulations were made imposing a dynamic water elevation at the ocean open boundary, admitting eleven tidal constituents (M_{SF}, O_1, K_1, N_2, M_2, S_2, MN_4, M_4, MS_4 and M_6). The impact of SLR in the lagoon was studied performing simulations with

MORSYS2D imposing different amplitudes of Z_0 (mean sea level) in agreement with elaborated SLR projections presented in Chapter 2.

The effects of wind and fluvial flow were despised because they have minor importance than the tidal forcing in the lagoon dynamics and morphodynmics. The median sediment grain size (d_{50}) used is variable in space and is based on data published by Freitas et al. (2005) and on sediments data collected in surveys performed in 2006 in the scope of the EMERA research project (Study of the Morphodynamic of the Ria de Aveiro Lagoon Inlet). The adopted sediment transport formula was given by Engelund-Hansen (Plecha et al., 2009). The bottom variation was computed admitting a porosity (λ) of 0.35.

The runs performed with MORSYS2D model were divided in two types consonant to the simulation durations. Short term simulations runs during sixty days were made to compute sediment fluxes in spring tide, neap tide and residual conditions, and long term simulations runs of six years and three months were made to depict long term bathymetric changes. In the overall simulations the time step of ELCIRC was ninety seconds. The adopted SAND2D time step's in short term simulations was one hour while in the long term simulations was twenty four hours.

3.4 – Characterization of lagoon hydrodynamics and inlet morphodynamics

3.4.1 – Present mean sea level

The characterization of lagoon hydrodynamics and inlet morphodynamics was carried out through short term simulations of sixty days with MORSYS2D. These simulations were performed running the model with numerical bathymetries based on local bathymetric surveys performed in June of 2001, September of 2005 and September of 2007. For each bathymetry, the sediment flux in a region near the inlet, and the tidal prism at the inlet and at the mouth of main channels were evaluated and analysed. Furthermore, it was made a long term simulation starting at June of 2001 and finishing at September of 2007. Results of this simulation were used to compute the sedimentation rates from the difference between predicted bathymetries. In order to analyse the model performance the computed sedimentation rates were compared with those calculated from the difference between observed bathymetries. Figure 3.5 shows the location of the cross-sections where the

sediments fluxes and tidal prism were evaluated and the regions where sedimentation rates were computed.

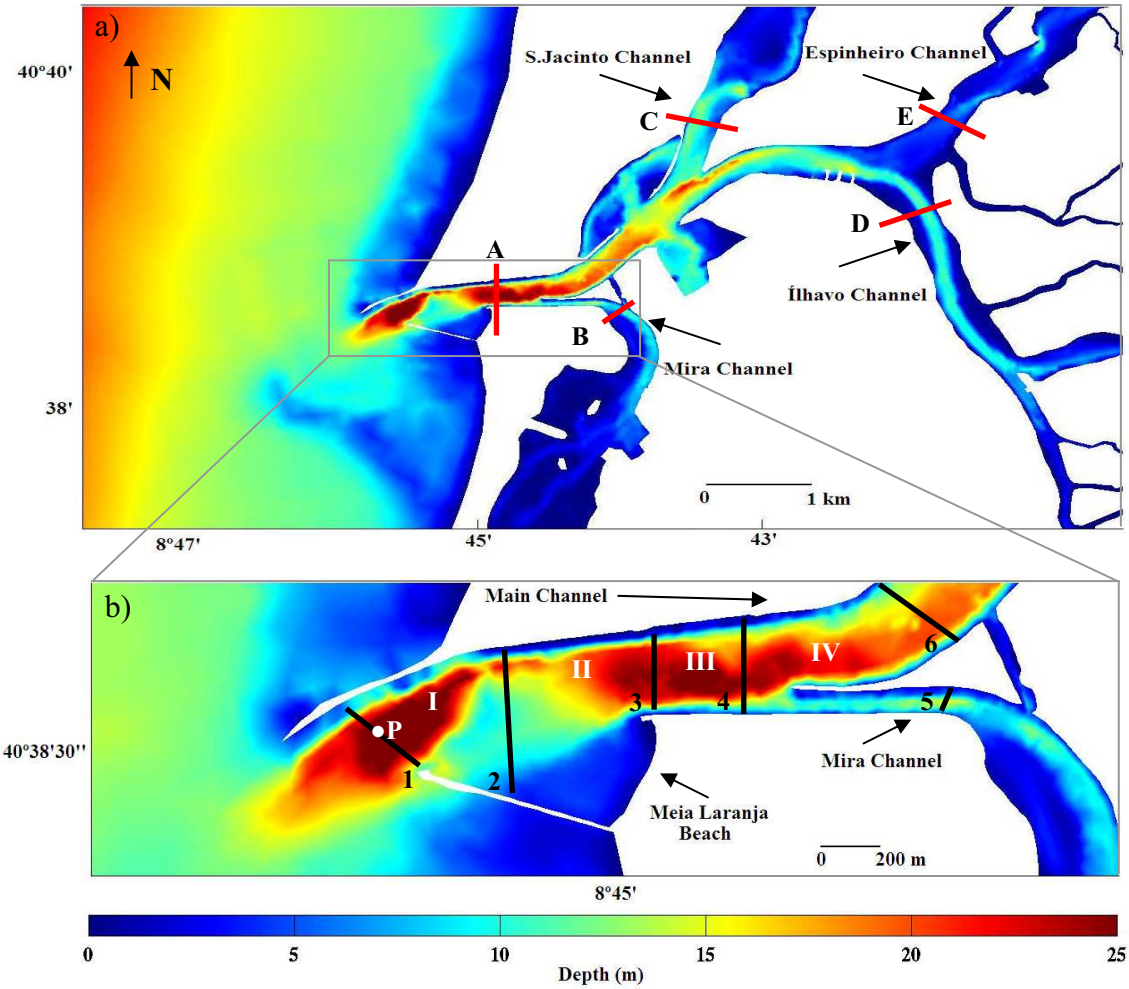

Figure 3.5 - Ria de Aveiro lagoon: a) Cross-sections location where tidal prism was evaluated (A to E); b) Cross-sections location where transport of sediments was computed (1 to 6) and regions where sedimentation rates were computed (I to IV). The point P represents a generic point where sea surface height and the sediment flux were analysed.

Figure 3.6 represents time series of sea surface elevation and of longitudinal and meridional sediments fluxes *(F_x* and *F_y* respectively) in a generic point P at the inlet of Ria de Aveiro (see Figure 3.5), for the 2001 bathymetry survey. The oscillations in sea surface associated with the diurnal inequality of tides generate strong differences on sediment transport, mainly in spring tide. The longitudinal flux is always greater than the meridional flux evidencing that transport is mostly longitudinal. Another important conclusion is that consecutive neap and spring tides generate very different sediment transports.

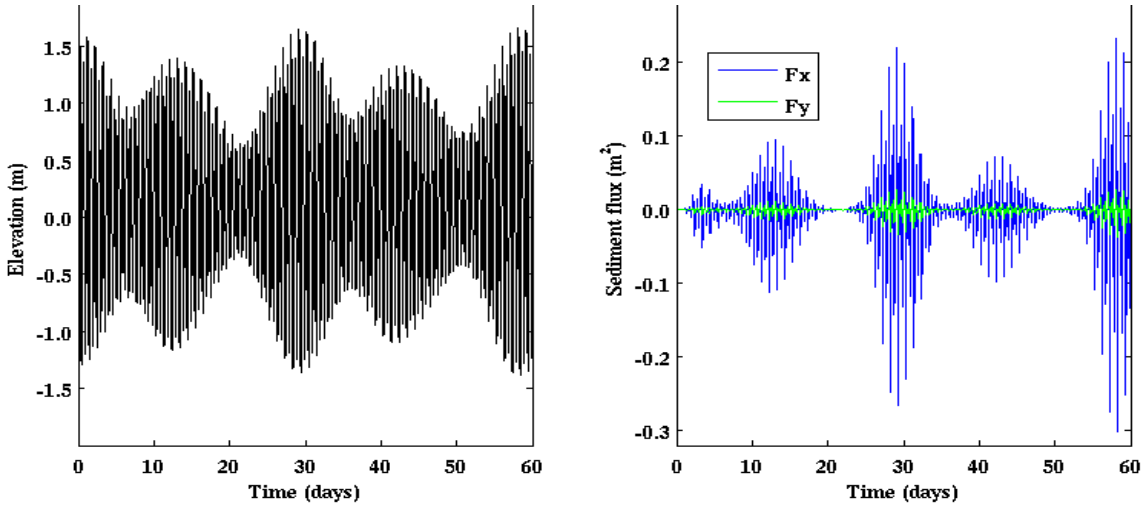

Figure 3.6 - Temporal evolution of sea surface height (left) and sediment flux (right), at a generic point in the inlet.

The sediments transport through the cross-sections represented in Figure 3.5 b) was computed, in order to identify regions with eroding and accreting trend and also to quantify the rate of erosion and deposition. Three distinct situations were analysed, spring tide, neap tide and residual. For each situation the transport into (V_{in},) and outward (V_{out}) cross-section was computed, as well as the budget. Negative values means that the transport is seaward, and positive values are landward. The sediments transport for the spring and neap tide were obtained identifying the maximum spring tide (3.0 m) and the minimum neap tide (0.9 m) of the short term runs, and averaging the sand fluxes during two M_2 tidal cycles (2×12.42 hours). The residual fluxes were obtained averaging the sand fluxes during two M_{SF} constituent periods (2×14.78 days). Table 3.1 presents these sediments transports for 2001, 2005 and 2007 bathymetric surveys. The results show that at neap tide the net sediment transport through all cross-sections is close to zero. The greatest transport rates were found on spring-tide, at cross-sections 2 and 6. The residual net transport is mostly seaward for all cross-sections. However, as the net sediment transport at the inlet cross-section is lower than the sum of the net sediments transports at cross-sections 5 and 6, there is deposition of sand in the region delimited by the inlet cross-section and cross-sections 5 and 6. The residual volume of sand deposited in this region was 72.7 m^3/day for 2001, 119.8 m^3/day for 2005 and 60.7 m^3/day for 2007.

Table 3.1 - Sediment transport (m^3/day) through cross-sections at extreme spring tide, neap tide and residual conditions.

Bathymetry	Cross-section	Spring tide			Neap tide			Residual		
		V_{in}	V_{out}	Budget	V_{in}	V_{out}	Budget	V_{in}	V_{out}	Budget
2001	1	66.7	-79.0	**-12.3**	0.5	-0.5	**0.0**	26.5	-30.5	**-4.0**
	2	403.2	-613.4	**-210.2**	3.3	-3.9	**-0.6**	167.7	-234.6	**-66.9**
	3	98.1	-167.4	**-69.3**	0.8	-1.1	**-0.3**	39.3	-64.3	**-25.0**
	4	102.9	-146.2	**-43.3**	0.8	-0.9	**-0.1**	41.0	-56.2	**-15.2**
	5	51.1	-70.5	**-19.4**	0.2	-0.4	**-0.2**	19.5	-46.4	**-26.9**
	6	143.2	-287.8	**-144.6**	1.3	-1.7	**-0.4**	58.7	-108.5	**-49.8**
2005	1	118.0	-120.9	**-2.9**	0.8	-0.8	**0.0**	32.8	-33.3	**-0.5**
	2	433.5	-632.1	**-198.6**	3.4	-4.4	**-1.0**	125.9	-175.3	**-49.4**
	3	214.8	-349.4	**-134.6**	1.8	-2.5	**-0.7**	61.8	-96.0	**-34.2**
	4	204.2	-292.2	**-88.0**	1.7	-2.0	**-0.3**	58.8	-81.4	**-22.6**
	5	151.8	-205.8	**-54.0**	0.9	-1.5	**-0.6**	43.3	-57.2	**-13.9**
	6	353.3	-769.2	**-415.9**	3.3	-5.0	**-1.7**	104.5	-210.9	**-106.4**
2007	1	95.5	-85.5	**10.0**	0.6	-0.6	**0.0**	26.1	-23.1	**3.0**
	2	485.3	-666.9	**-181.6**	3.8	-4.0	**-0.2**	138.4	-176.6	**-38.2**
	3	136.3	-169.5	**-33.2**	1.1	-1.1	**-0.0**	38.5	-46.1	**-7.6**
	4	135.2	-161.8	**-26.6**	1.0	-1.0	**0.0**	37.9	-44.1	**-6.2**
	5	116.9	-176.8	**-59.9**	0.6	-1.5	**-0.9**	31.7	-49.9	**-18.2**
	6	244.3	-412.8	**-168.5**	2.3	-2.6	**-0.3**	70.9	-110.4	**-39.5**

The residual flux is represented in Figure 3.7 for the 2001 bathymetric survey. A similar calculus was made for the other bathymetric surveys, but the observed patterns are similar to this one and, therefore, are not presented here. It was observed that the residual flux is nearly always seaward; the exceptions are at the head of the south jetty and in the upper part of the Main channel. The pattern observed suggests that there is accretion on the mouth of Mira and Main channels, as well as near the inlet, given that there is an accented decrease of the sediments fluxes in these regions. On the other hand, downstream the inlet cross-section the pattern suggests erosion, because it is observed a strong decrease of the sediments fluxes. Figure 3.5 shows that in the accreting regions the depth increases suddenly and in the eroding region near the lagoon mouth occurs the opposite, a sudden depth decrease.

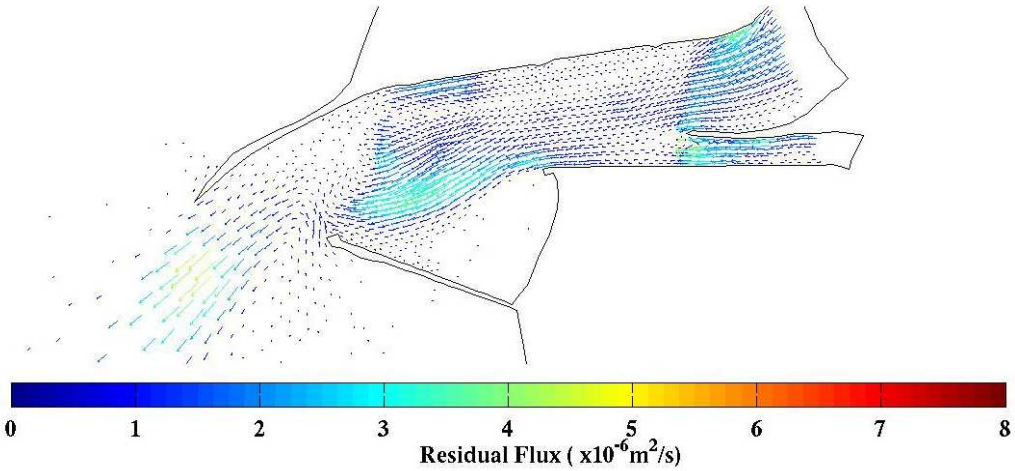

Figure 3.7 - Residual sediment flux (m^2/s) field at Ria de Aveiro inlet for 2001 bathymetry survey.

In order to evaluate the model's ability to reproduce the bathymetric changes observed in reality, the sedimentation rates in the regions (I – IV) represented on Figure 3.5 were computed from the difference between bathymetries, both observed and prdicted (long term). Results are presented in Table 3.2, and reveal that, between June of 2001 and September of 2007, there was accretion in every region, but the model predicts accretion only on regions I and IV. In these cases the observed sedimentation rate is greater than the predicted.

Table 3.2 - Sedimentation rate (m^3/day) between cross-sections from 2001 to 2005 and from 2001 to 2007 both observed and predicted.

Period	Region	Sedimentation rate (m^3/day)	
		Observed	Predicted
2001/2005	I	+92.2	+39.6
	II	+135.6	-29.4
	III	+68.2	-4.9
	IV	+149.4	+54.9
2001/2007	I	+104.4	+30.9
	II	+147.4	-23.2
	III	+55.5	-3.1
	IV	+146.8	+45.6

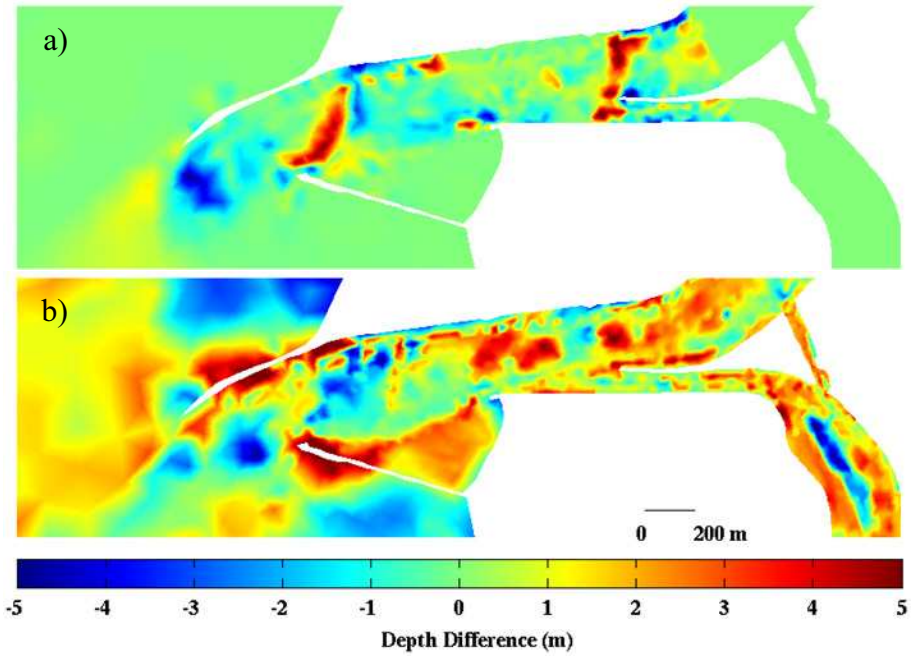

Figure 3.8 - Depth difference field between bathymetries of June of 2001 and September of 2005, a) predicted and b) observed.

To perceive the differences between observed and predicted sedimentation rates, the difference between observed and predicted bathymetries was represented. Figure 3.8 shows the differences between the bathymetries of 2001 and 2005, both predicted and observed. The difference field between 2001 and 2007 bathymetries was also represented, however its pattern is similar, and therefore is not presented here.

The effect of waves is not accounted for these simulations. This limitation can explain some of the differences between observed and predicted bathymetries, mainly in the inlet adjacent zone. Some accreting areas are not well reproduced by the model, namely near the north and south jetties, and close to Meia Laranja beach. An analysis of the cross sectional bathymetry near the northern breakwater was made (not shown), and reveals that the pronounced bathymetric changes are observed within a strip of around 50 m close to the structure. The changes are probably justified by the presence of structural rocks that collapsed from the breakwater and by the emergency works performed in 2004 to repair this structure. Indeed these works deposited large amount of rocks at the breakwater and near its bottom, which were observed in recent side sonar images. So, this trend can't be understood as a flaw of the model. The strong accretion observed near the south jetty has also an explanation. The bathymetric survey performed in June of 2001 has some data fault near the south jetty. Consequently, the adopted depth when there is data fault is the depth

observed in a bathymetric survey performed during 1987/88. So, the 5 m of difference depth observed don't correspond to the accretion observed during four years and three months, but corresponds to the accretion observed in about eighteen years. This analysis evidences that the sedimentation rates presented in Table 3.2 computed from the difference of observed bathymetries, and referring to region I, can not be directly compared with the model results.

The accreting trend observed upstream cross-section 3 (Figure 3.5) is not well reproduced by the model. While the model reproduces accretion essentially near the bifurcation of the main channel, the observed trend indicates that there is accretion in this entire region. However there are trends well reproduced by the model, namely the erosive trend observed downstream the inlet and the accreting trend upstream the inlet (north of south jetty), followed by erosion.

The deviation between observed and predicted bathymetries pointed out for some regions suggests doubts about the usefulness of the long-term simulations performed with MORSYS2D. To appraise the worth of these simulations, the relative deviations between the bathymetry observed in 2005 and the bathymetries observed in 2001 (Er_1) and predicted for 2005 (Er_2), were computed for each grid element of the morphodynamic domain by:

$$Er_1(\%) = \frac{\left|Hobs_{05} - Hobs_{01}\right|}{\left|Hobs_{05}\right|} \times 100 \qquad (3.1)$$

$$Er_2(\%) = \frac{\left|Hobs_{05} - Hsim_{05}\right|}{\left|Hobs_{05}\right|} \times 100 \qquad (3.2)$$

Where $Hobs_{05}$ and $Hobs_{01}$ are the observed depth in 2005 and 2001 respectively, and $Hsim_{05}$ is the predicted depth of 2005. If Er_1 is greater than Er_2, it means that the bathymetry predicted for 2005 deviate less from the bathymetry observed for 2005 than the initial bathymetry of 2001. So, the condition $Er_1 > Er_2$ indicates that the long term morphodynamic simulations are useful. The opposite condition indicates that it is not advantageous to update the bathymetries. The values computed for Er_2 and Er_1 are presented in Figure 3.9. Both patterns are similar, however the greatest deviations (>40%) are found in Meia Laranja beach and close to the north margin of the main channel.

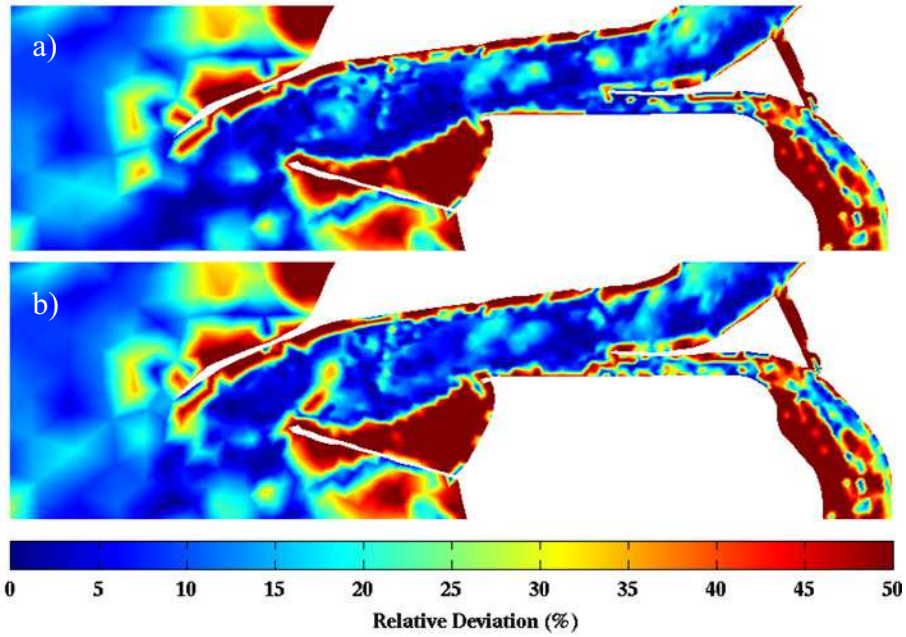

Figure 3.9 – Relative error (%) between bathymetries. a) Er_1 and b) Er_2.

The difference field between Er_2 and Er_1 is presented in Figure 3.10. The grey colour represents the condition $Er_2 \geq Er_1$, indicating that it is disadvantageous to update the bathymetry, while the overall colours represent $Er_2 < Er_1$.

Figure 3.10 shows that northward to the north jetty the flaws of MORSYS2D are evident, and can be explained by the omission of wave forcing and data fault. On the other hand, inside the lagoon there are several regions where it is advantageous to perform the bathymetry updates, namely upstream cross-section 3 (see Figure 3.5).

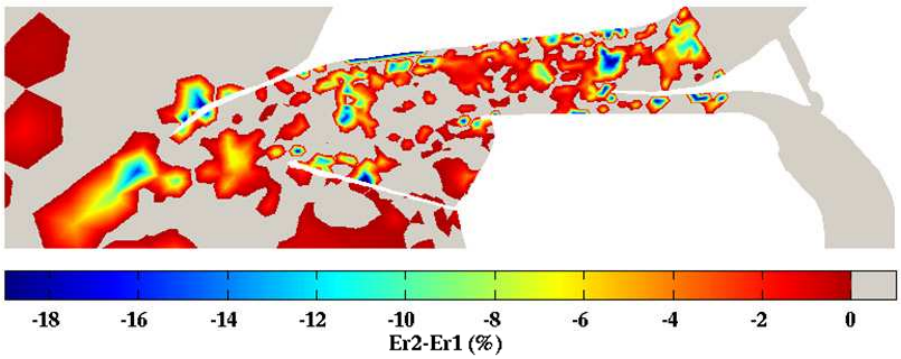

Figure 3.10 - Difference field between Er_2 and Er_1.

Considering that the error, Er_2, around the jetties can't be understood as a defect of the model, and that this study is devoted to the characterization of morphodynamics upstream

the inlet, the predictions performed by MORSYS2D are useful in order to obtain more reliable results. However, it has to be account that MORSYS2D results have some limitations, namely in Meia Laranja beach.

The tidal prism was evaluated at the cross-sections represented on Figure 3.5 a), from the output of the hydrodynamic model, based on observed and predicted bathymetries, under spring and neap tide conditions. The tidal range is about 3.2 m for spring tide and 0.4 m for neap tide. Cross-section A is representative of the inlet, and cross-sections B, C, D, and E represent the mouth of the four main channels of Ria de Aveiro. These results are presented in Table 3.3.

Table 3.3 - Tidal prism (m^3) at spring tide and neap tide conditions both from observed and predicted bathymetries.

Bathymetry	Cross-section	Tidal Prism ($\times 10^6$ m^3)			
		Observed		Predicted	
		Spring Tide	Neap Tide	Spring Tide	Neap Tide
2001	A	87.5	28.9		
	B	11.8	3.7		
	C	38.8	13.6		
	D	8.2	2.5		
	E	20.2	6.9		
2005	A	85.3	28.3	87.2	28.9
	B	11.1	3.5	10.8	3.7
	C	38.8	13.8	38.8	13.6
	D	7.5	2.3	8.2	2.5
	E	20.5	7.0	20.6	7.0
2007	A	78.8	26.1	87.0	28.7
	B	10.0	3.1	11.9	3.7
	C	33.2	11.9	38.8	13.6
	D	7.4	2.2	8.2	2.5
	E	21.5	7.3	20.2	6.9

The results based on the observed bathymetries show a decrease of the tidal prism of about 10% for all cross-sections (except section E) between 2001 and 2007. A study performed by Araújo et al. (2008) indicates that a decrease in the inlet depth leads to a decrease in the tidal amplitude and consequently to a decrease in tidal prism. An analysis of the mean

depth observed at the cross-section A for the period 2001-2007 revealed that it decreased about 1.5 m, justifying the decrease found for the tidal prism.

It can be observed, that there is a good agreement between tidal prisms computed from observed and predicted bathymetries. For the 2005 bathymetry, the maximum error between tidal prisms computed from observed and predicted bathymetries is 2%, while for the 2007 bathymetry the maximum error increases to 10.5%.

The tidal prism for each of the main channels relative to its value at the inlet is about 13% for Mira channel, 45% for S. Jacinto channel, 9% for Ílhavo channel and 25% for Espinheiro channel. Comparing to tidal prisms reported by Dias (2001) and determined using the SIMSYS2D model and a bathymetry based on surveys from 1987/88, the absolute value at the inlet was found to be about 1.5 times higher than the estimated here. However, the percentage of distribution for the other channels is similar; the major difference is found for S. Jacinto channel, with values 10% higher. Given that the tidal ranges considered in these estimates are similar to those used in the estimates by Dias (2001), it suggests that the differences found in tidal prisms are associated with the bathymetry, namely with a depth decrease at the lagoon mouth.

The comparison with the tidal prisms values estimated by Picado (2008) using the ELCIRC model and a bathymetry based on a general survey from 1987/88 but updated with the results of more recent surveys close to the lagoon mouth, revealed good agreement between absolute values and percentages in all these cross-sections.

3.4.2 – Changes induced by a mean sea level rise

The analysis of future conditions was carried out through long term simulations, with a duration of six years and three months as before, and considering different mean sea levels correspondent to the different SLR scenarios previously determined. The bathymetry of 2001 was chosen to initialize the runs with MORSYS2D because it is unknown how will be the bathymetry at the end of this century. It will be possible to project a bathymetry attending to the sedimentation rates computed from the differences between observed bathymetries. However, as it is discussed before, the sedimentation rates for the region I account the structural rocks that have collapsed from the breakwater and therefore, don't include only sand. On the other hand if these rates are extrapolated, apart the future

dredging operations and possible changes in the inlet configuration the system behaves non-linearly and therefore those projections will be inadequate.

The projections presented in Chapter 2 revealed an increase in mean sea level between 0.25 m under scenario B1 and 0.34 m under scenario A2. As the difference between these values is 0.09 m, the analysis performed for future conditions of the lagoon disregards scenario A1B and considers only the extreme scenarios A2 and B1.

As for the actual conditions, residual transports of sediments at the same cross-sections were computed considering the same integration periods, but admitting a mean sea level 0.34 m (A2 scenario) or 0.25 m (B1 scenario) higher than the present. The results are present in Tables 3.4 and 3.5. Comparing these results with those presented previously in Table 3.1 are detected morphodynamic changes due to the increase in sea level.

Table 3.4 - Sediment transport (m^3/day) through cross-sections at extreme spring tide, neap tide and residual conditions, for scenario A2.

Bathymetry	Cross-section	Spring tide			Neap tide			Residual		
		V_{in}	V_{out}	Budget	V_{in}	V_{out}	Budget	V_{in}	V_{out}	Budget
2094	1	184.0	-196.9	**-12.9**	2.3	-2.0	**0.3**	57.7	-58.4	**-0.7**
	2	1057.3	-1472.6	**-415.3**	15.8	-14.6	**1.2**	346.4	-431.4	**-85.0**
	3	268.3	-417.6	**-149.3**	3.5	-4.4	**-0.9**	83.9	-123.1	**-39.2**
	4	282.7	-371.9	**-89.2**	3.6	-3.8	**-0.2**	88.2	-110.2	**-22.0**
	5	129.5	-164.3	**-34.8**	1.2	-1.7	**-0.5**	38.8	-49.4	**-10.6**
	6	396.2	-760.1	**-363.9**	5.8	-6.8	**-1.0**	126.8	-218.9	**-92.1**
2098	1	159.0	-190.8	**-31.8**	2.1	-2.0	**0.1**	50.3	-56.6	**-6.3**
	2	912.1	-1196.0	**-283.9**	13.3	-12.5	**0.8**	296.7	-354.1	**-57.4**
	3	315.0	-393.2	**-78.2**	4.1	-4.1	**0.0**	102.7	-116.3	**-13.5**
	4	316.5	-421.4	**-104.9**	4.0	-4.4	**-0.4**	100.1	-124.8	**-24.7**
	5	142.3	-167.8	**-25.5**	1.3	-1.9	**-0.6**	42.7	-51.2	**-8.5**
	6	448.1	-911.9	**-463.8**	6.5	-7.8	**-1.3**	141.9	-258.6	**-116.7**
2100	1	133.1	-199.6	**-66.5**	1.7	-1.9	**-0.2**	41.9	-58.8	**-16.9**
	2	811.6	-1129.4	**-317.8**	11.9	-11.8	**0.1**	265.7	-337.7	**-72.0**
	3	357.9	-435.3	**-77.4**	4.8	-4.4	**0.4**	117.1	-128.8	**-11.7**
	4	351.1	-495.2	**-144.1**	4.5	-5.0	**-0.5**	111.3	-147.1	**-35.6**
	5	118.8	-158.5	**-39.7**	1.0	-1.7	**-0.7**	35.5	-48.4	**-12.9**
	6	441.6	-876.3	**-434.7**	6.3	-7.7	**-1.4**	140.1	-250.8	**-110.7**

Table 3.5 – Sediment transport (m^3/day) through cross-sections at extreme spring tide, neap tide and residual conditions, for scenario B1.

Bathymetry	Cross-section	Spring tide			Neap tide			Residual		
		V_{in}	V_{out}	Budget	V_{in}	V_{out}	Budget	V_{in}	V_{out}	Budget
2094	1	155.9	-172.1	**-16.2**	1.8	-1.6	**0.2**	47.9	-50.1	**-2.2**
	2	906.4	-1298.7	**-392.3**	12.1	-11.7	**0.4**	290.9	-374.0	**-83.1**
	3	227.8	-365.3	**-137.5**	2.7	-3.5	**-0.8**	69.8	-105.7	**-35.9**
	4	239.5	-323.6	**-84.1**	2.8	-3.0	**-0.2**	73.3	-94.0	**-20.7**
	5	113.0	-147.1	**-34.1**	0.9	-1.3	**-0.4**	33.2	-43.2	**-10.0**
	6	335.0	-657.6	**-322.7**	4.5	-5.4	**-0.9**	105.2	-185.5	**-80.3**
2098	1	136.1	-166.9	**-30.8**	1.6	-1.5	**0.1**	42.2	-48.7	**-6.5**
	2	780.5	-1037.4	**-256.9**	10.2	-9.7	**0.5**	248.0	-301.7	**-52.7**
	3	277.9	-346.4	**-68.5**	3.2	-3.2	**0.0**	87.4	-100.6	**-13.2**
	4	273.9	-371.5	**-97.6**	3.1	-3.5	**-0.4**	84.5	-108.0	**-23.5**
	5	124.2	-149.3	**-25.1**	1.0	-1.5	**-0.5**	36.4	44.5	**-8.1**
	6	377.8	-790.2	**-412.4**	5.1	-6.2	**-1.1**	117.7	-220.2	**-102.5**
2100	1	114.8	-182.7	**-67.9**	1.3	-1.6	**-0.3**	35.3	-52.7	**-17.4**
	2	688.9	-999.2	**-310.3**	9.2	-9.5	**-0.3**	220.8	-292.3	**-71.5**
	3	316.3	-394.2	**-77.9**	4.1	-3.6	**0.5**	100.3	-112.6	**-12.3**
	4	306.0	-447.3	**-141.3**	3.6	-4.0	**-0.4**	94.6	-126.7	**-32.1**
	5	97.8	-132.1	**-34.3**	0.8	-1.2	**-0.4**	28.5	-39.0	**-10.5**
	6	377.2	-763.7	**-386.5**	4.9	-6.2	**-1.3**	117.3	-215.5	**-98.2**

It is clear that the rise in sea level leads to an increase in sediments transport into and outward cross-sections for the overall conditions analysed. The only exception is found in section 5, where the volumes into and outward cross-section are similar.

The sediment transport trends for residual conditions in each cross-section are represented in Figures 3.11, 3.12 and 3.13. It is evident from Figures 3.11 and 3.12 that the sediments transport rates increase with the increase in mean sea level. The SLR scenario A2 induces higher sediments transport than scenario B1, however the net sediment transport doesn't varies significantly with scenarios (see Figure 3.13). The biggest net transport deviation between scenarios is found in cross-section 6 where the export of sediments under scenario A2 is about12% higher than from scenario B1. The analysis of Figure 3.13 reveals that the increase in mean sea level induces changes in the net sediment transport in each cross-

section, except at the section 3 where the mean net transport don't varies significantly between present mean sea level and SLR scenarios.

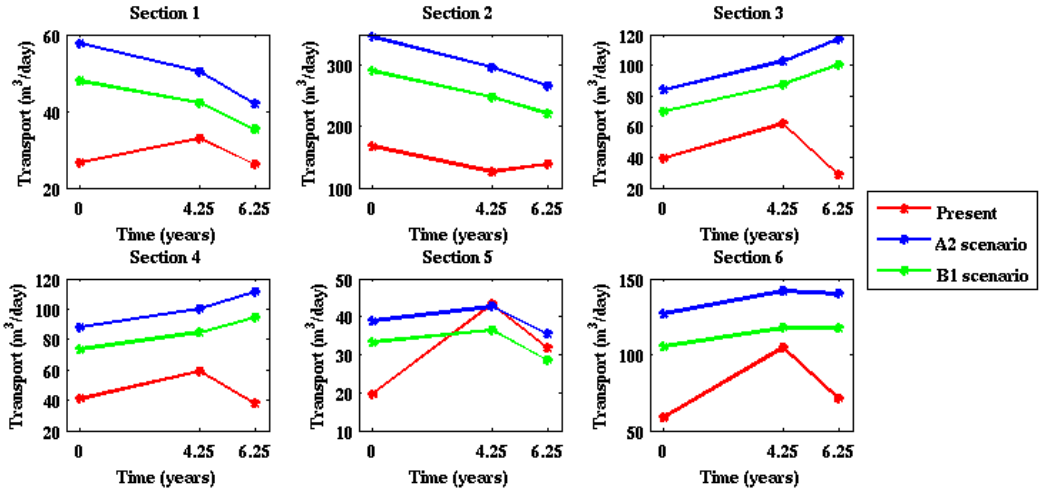

Figure 3.11 – Residual sediment transport trend into cross-sections, for present mean sea level and for the sea level rise scenarios A2 and B1.

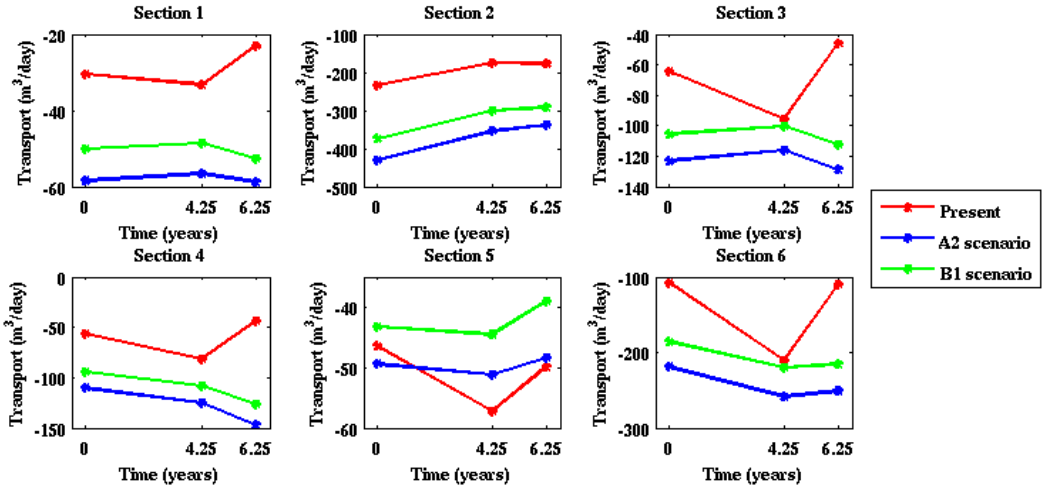

Figure 3.12 – Residual sediment transport trend outward cross-sections, for present mean sea level and for the sea level rise scenarios A2 and B1.

On average, in sections 1, 2, 4 and 6 the residual transports become more negative for SLR scenarios than for present mean sea level and therefore the lagoon exports more sediments. In Figures 3.11, 3.12 and 3.13 it is evident at some sections that the present transport trends aren't identical to those projected for the future. This is natural because the present trends are based on observed bathymetries, and the future trends are based on predicted

bathymetries and it was already pointed out the limitations of the present application of MORSYS2D.

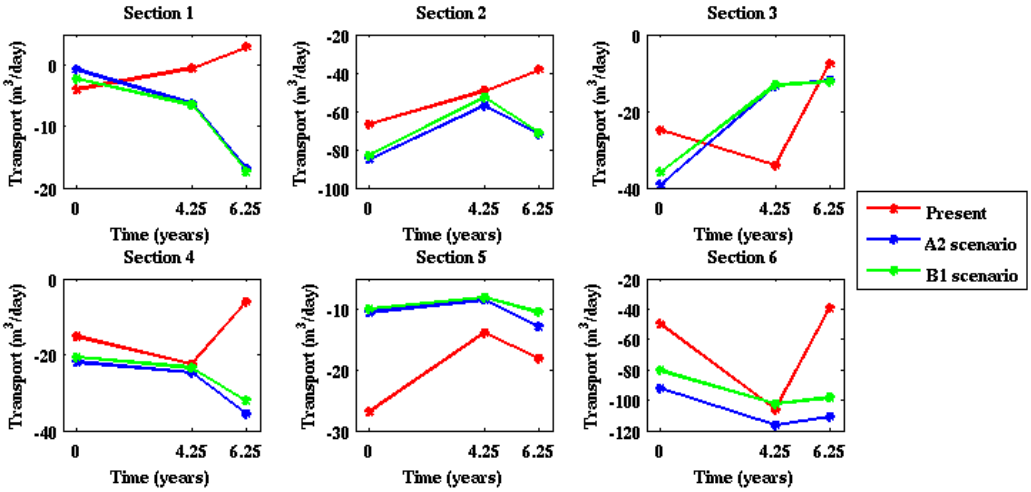

Figure 3.13 – Residual net sediment transport trend, for present mean sea level and for the sea level scenarios A2 and B1.

In general, the net sediment volume in each cross-section tends to increase, and cross-section 6 presents the highest increase. This means that there is a trend to increase the accretion inside the domain, considering that the input of sediments increases more than the output at the inlet. The amount of residual sand deposited in the overall domain is greater for SLR scenarios. Under SLR scenario A2 the deposited sand increased on average about 29% related with present conditions, while for scenario B1 the increase is less emphasized, with a value around 12.2%.

Figure 3.14 represents the residual flux for SLR scenarios A2 and B1. Comparing this figure with Figure 3.7 it is detected that the pattern of residual flux don't change with SLR, however it is evident an intensification of the residual flux for both SLR scenarios, specially for the SLR scenario A2. This intensification was quantified by calculating the difference of residual fluxes between SLR scenarios and present conditions (Figure 3.15). In the regions where the sediment fluxes are higher there was an increase in the intensity of the residual fluxes of about 50% for A2 SLR scenario and 40% for SLR scenario B1. For the overall morphodynamic domain the increase in the residual fluxes was about 90% for SLR scenario A2 and 65% for SLR scenario B1.

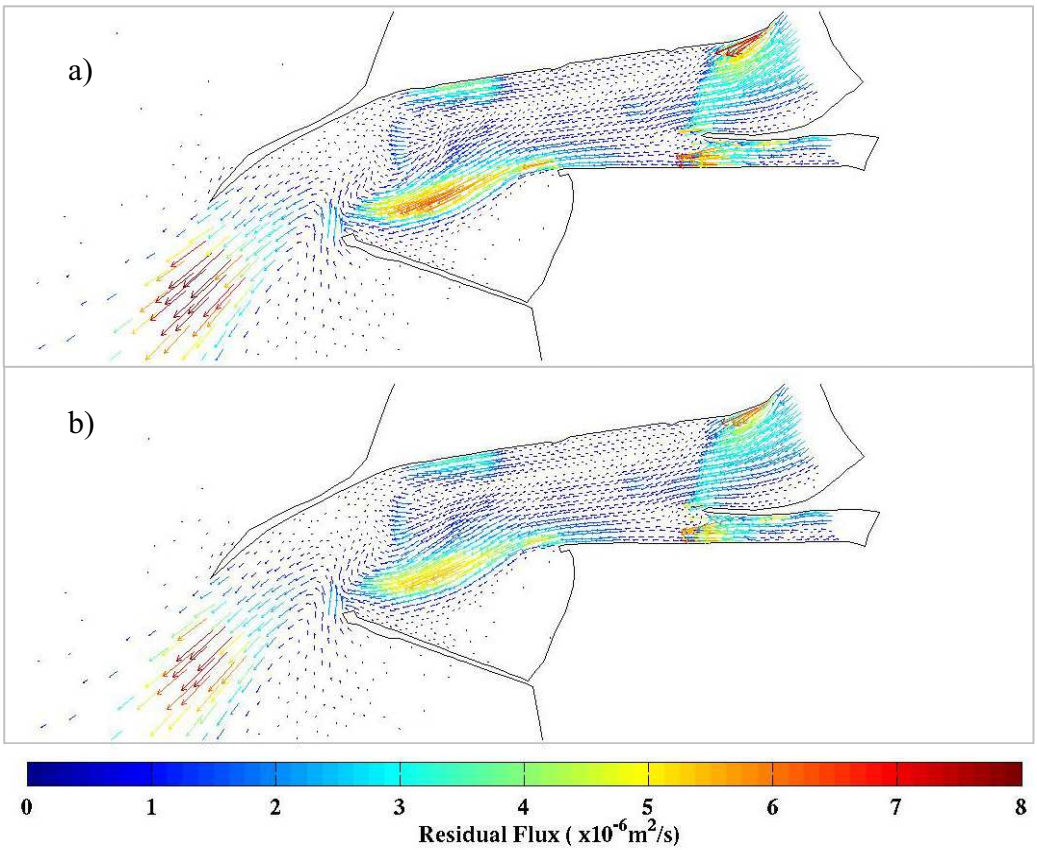

Figure 3.14 - Residual sediment flux fields for SLR scenarios: a) A2 and b) B1.

The sedimentations rates between 2096 and 2100 were also computed from the difference of bathymetries in the same four regions defined before (Figure 3.5) and are presented in Table 3.6. Figure 3.16 represents sedimentation rates computed from predicted bathymetries both for present mean sea level and SLR scenarios A2 and B1. Comparing these sedimentation rates, it is verified that the trend of sedimentation rates computed for the present mean sea level is maintained but its intensity increases: region IV presents the highest changes, with an increase in the accreting rate of about 88% for both SLR scenarios

Take into account the mismatch between sedimentation rates computed from predicted bathymetries and those computed from the observed bathymetries it is supposed that the projected erosive trend at region II is not realistic, and for the other regions the accretion rates are probably higher than those projected.

The tidal prism was also estimated under SLR scenarios for the same cross-sections illustrated on Figure 3.5. It is verified that the tidal prism don't varies significantly between 2096 and 2100, therefore only the values for a single year (2100) are presented in Table 3.7

as representative of the entire period. An analysis of the predicted bathymetries for this period revealed that the mean depth at the cross-section A only varies 0.3 m, for both scenarios. This weak variation of mean depth explains why the tidal prism remains nearly unchanged during this period.

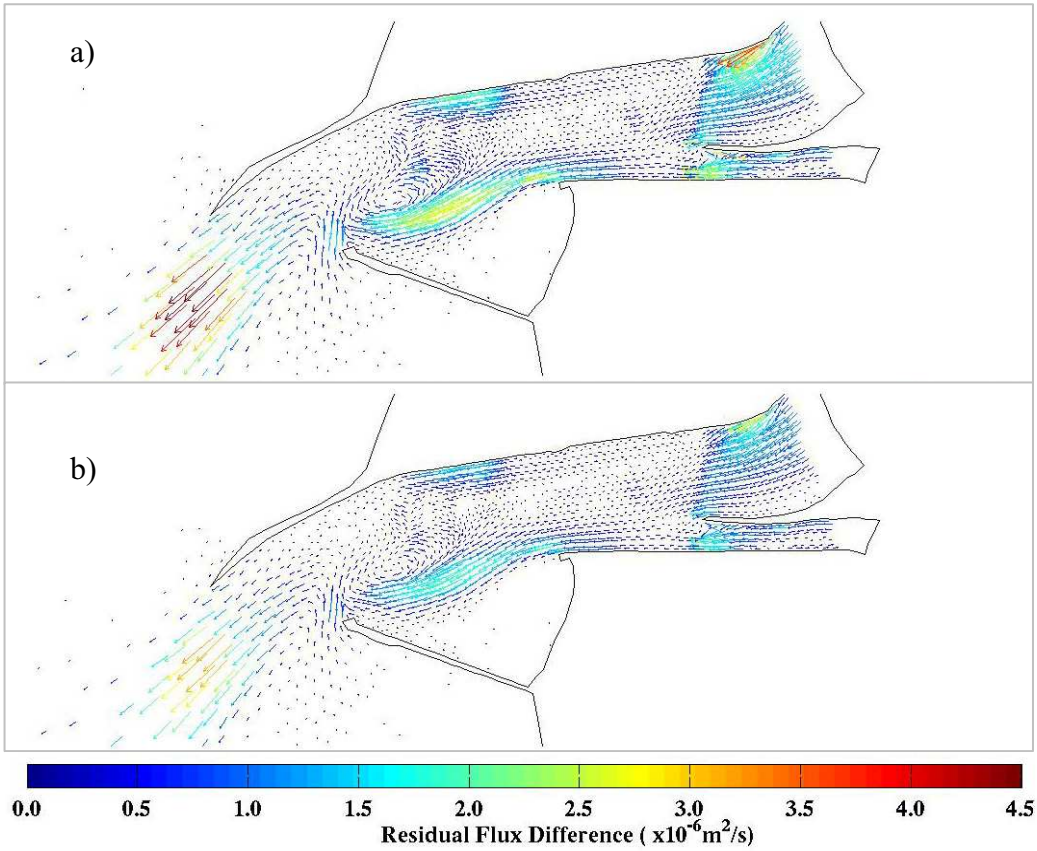

Figure 3.15 - Difference fields between residual sediment fluxes for present mean sea level and SLR scenarios: a) A2 and b) B1.

Table 3.6– Sedimentation rate (m^3/day) between cross-sections between 2094 and 2100 for SLR scenarios A2 and B1.

Period	Region	Sedimentation rate (m^3/day)	
		A2 scenario	B1 scenario
2094/2100	I	+37.5	+37.5
	II	-32.6	-32.6
	III	+2.5	+2.6
	IV	+85.8	+85.9

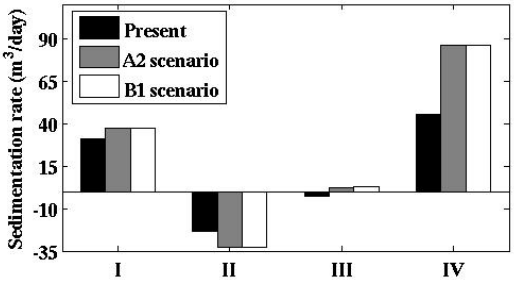

Figure 3.16 - Sedimentation rates computed from predicted bathymetries for present mean sea level and for SLR scenarios A2 and B1.

Table 3.7– Projected tidal prisms (×10^6 m^3) at neap tide and spring tide conditions under SLR scenarios A2 and B1.

		A2 scenario		B1 scenario	
Bathymetry	**Cross-section**	**Spring Tide**	**Neap Tide**	**Spring Tide**	**Neap Tide**
2100	A	105.2	36.9	101.2	36.9
	B	14.4	4.9	13.7	4.9
	C	47.8	17.4	45.5	17.4
	D	9.7	3.2	9.3	3.2
	E	25.2	9.3	23.9	9.3

Figure 3.17 shows the tidal prism evolution in each cross-section for both situations analysed, admitting that the tidal prism for the present mean sea level in each cross-section is the tidal prism computed from the observed bathymetry of 2007. The projected tidal prisms indicate an increase for both SLR scenarios for all cross-sections from the present until 2100. The tidal prism at the inlet increased about 28% for SLR scenario A2 and 23% for SLR scenario B1 relative to the tidal prism of 2007.

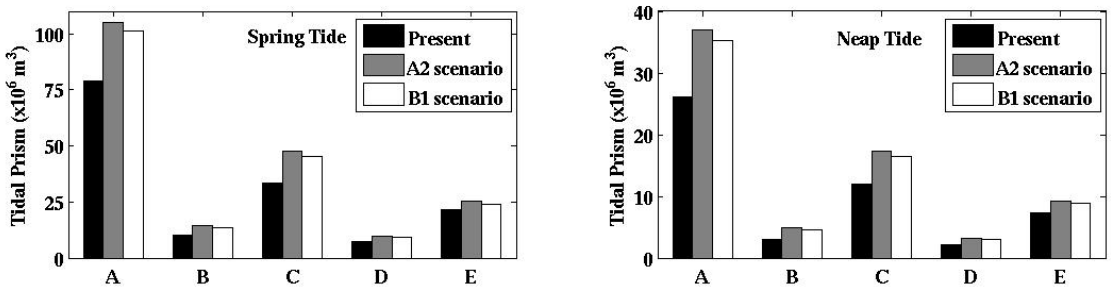

Figure 3.17 - Tidal prism in each cross-section for spring tide (left) and neap tide (right) conditions.

3.5 – Limitations of morphodynamic predictions

As described along this chapter there are several uncertainties associated with the simulations performed with MORSYS2D in order to characterize the present conditions of the lagoon and to project the changes induced by the sea level rise. The physical characteristics of sediments, the ambiguities in the forcings and in the sediment transport formulae were pointed out by Fortunato et al. (2009) as the principal sources of uncertainty related with morphological predictions.

The median sediment grain size (d_{50}) used is variable in space and is based on data collected from surveys. However, the distribution of bottom sediments in Ria de Aveiro inlet is still poorly known and the rare information indicates that it is very heterogeneous, combining fine, median and coarse sediment fractions (Martins et al., 2007). So, a better understanding of physical characteristics of sediments can be useful to obtain more exact results.

Another important source of error comes from the forcing specification. In the simulations presented here the effect of waves was omitted, due to computational limitations. However, the inlet adjacent zone is subject to a highly energetic wave climate, very important in the transport of sediments (Plecha et al., 2007). The analysis of results has showed a difference between observed and predicted bathymetries in the areas where the effect of waves is more important.

The major source of uncertainty in morphodynamic simulations comes probably from the transport formulae. Plecha et al. (2009) have demonstrated that the transport formulation of Engelun-Hansen (1967) is the one that best describes the morphodynamic changes driven by tides in Ria de Aveiro inlet. However, the choice of the more suitable transport formulae is not a trivial task and is limited by the unavailability of good quality bathymetric data and by the insufficient frequency of measurements (Fortunato et al., 2009).

4 – Conclusions

This work reports the potential impacts of SLR on the hydrodynamics of Ria de Aveiro lagoon and on morphodynamics of this inlet. For that, projections of SLR were performed for the end of this century, based on the output of an AOGCM, the GISS-ER model. In spite of the several limitations in climate modelling mentioned in Chapter 2, the presented projections are within the range of other estimates performed by other scientists based on the extrapolation of observed data. This work also suggests a way for new research about local SLR projections for Portugal (or other countries), considering for example all AOGCM's used on IPCC report instead of using only the GISS-ER model. Or, on the other hand, to choose models with better spatial resolution. The study about local SLR projections has also contributed, for a better understanding of the factors that affect SLR in the Portuguese coast. The volume change and the exchange of water between ocean and other reservoirs are responsible to local SLR. The effect of land subsidence is weak when compared to the other effects.

The characterization of lagoon hydrodynamics and inlet morphodynamics for present mean sea level was carried out successful applying the morphodynamic model MORSYS2D to the lagoon and comparing the results of simulations with observed bathymetric data. This study has contributed to a better knowledge about the sediments dynamics in the inlet adjacent area. From the analysis performed it was concluded that the residual transport of sediments is mostly seaward, however the sediments tend to remain inside the lagoon due to the weak residual transport through the inlet cross-section. Furthermore, the transport of sediments in extreme neap tide is close to zero, contrasting with the strong transport of sediments in extreme spring tide. The observed bathymetry globally shows an accreting trend in the domain analysed. Nevertheless the model underestimates the observed accreting trend. The deviations between predicted and observed bathymetries around the inlet and outside the lagoon can be partially explained by the omission of wave forcing, which has significant influence on the sediments dynamics in this area. On the other hand, the deviations around the north jetty and in the north margin of main channel can be partially explained by the collapse of structural rocks from the jetty and by the works

performed to repair the structure and therefore can't be understood as a malfunction of the model .

From the comparison between the simulations performed with MORSYS2D for SLR scenarios and those for present mean sea level it is concluded that the transport of sediments increases with SLR, as well as the accretion inside the lagoon. The pattern of residual fluxes doesn't change for the SLR scenarios; however it is observed an intensification of the sediment fluxes for both scenarios comparing with the present situation. On average, it is verified an increase in residual fluxes of about 90% for SLR scenario A2 and 65% for SLR scenario B1. Although the residual fluxes of sediments increase more for SLR scenario A2 than for SLR scenario B1, the sedimentation rates between 2094 and 2100 are identical for both SLR scenarios. This fact suggests that there is more accretion in the accretion areas and at the same time more erosion in the erosion areas, for SLR scenario A2 than for SLR scenario B1.

As referred before, the morphodynamic projections have same limitations that may be overcome in the future. A better knowledge of physical characteristics of sediments will offer better boundary conditions and consequently more reliable results. A better quality of bathymetric data and more frequent bathymetric surveys will be useful to obtain more exact sedimentation rates, leading to better results with MORSYS2D. Another way to improve the projections will be to include the effect of waves in simulations and run the MORSYS2D in parallel in order to reduce the computational time. It is supposed that the divergence between predictions and observations at Meia Laranja beach can be partially explained by the omission of wave forcing. The interaction of waves with the breakwaters generates complex wave patterns that can be important in this area.

The uncertainty in projection results will be reduced if a future bathymetry could be projected for 2096 to better initialize the future runs: however this task is extremely hard and uncertain because the sedimentation trends are non-linear in time and also depend on the human action.

The hydrodynamics of the lagoon was also changed due to the increase in sea level. In this study it is only analysed the tidal prism. It is estimated an increase in tidal prism at the mouth of about 28% for SLR scenario A2, and 22% for SLR scenario B1 relative to tidal prism of 2007. The tidal prism projections reported here deviates from Silva and Duck (2001) estimates. They have projected an increase in tidal prism of about 22% for an

increase of 0.1 m in mean sea level. This deviation between projections is maybe due to the omission of the inundation of salt marsh and salt pans, in the projections reported here. Silva and Duck (2001) have included this effect from using aero-photogrammetric survey performed in 1987. So, in the future will be interesting to analyse and to identify the areas that will potentially inundate for the SLR scenarios reported here, considering for that the topographic data for the lagoon margins. This task will open conditions to evaluate other hydrodynamic consequences of SLR in the lagoon, namely the expected increase in salinity, intensity of currents, and sea surface elevation.

In this work, the waves, the river runoff, the wind and the precipitation were despised because these forcing have minor importance than the tides in the hydrodynamics of the lagoon. However, recent studies revealed that these forcing will potentially be changed in result of climate change, and the seasonal variations will be more emphasized than in the actuality. Cunha et al. (2006) estimated an increase of the precipitation seasonal asymmetry resulting essentially of a decrease in summer precipitation. Consequently, this change in the precipitation pattern will alter the river runoff pattern. Andrade et al. (2006) also projected a markedly seasonal pattern in waves associated with an increase in storminess. So, in the future it will be important to evaluate the impacts of these overall seasonal variations in the physical parameters of the lagoon, in order to prevent potential hazards, like the consequences of storm surges and flooding in the winter.

Another factor that was despised in this work was the man action. There is no doubt that this aspect will be the more important in the evolution of the lagoon, such as it was in the past. However, the consequences of the man in the lagoon are highly uncertain and long-term unpredictable. The trends determined for the lagoon can be changed every time by the man action and the projections reported here could make no sense in the future.

5 – References

Andrade, C., Pires, H. O., Taborda, R., Freitas, M.C. (2006). Zonas Costeiras. Alterações Climáticas em Portugal Cenários, Impactos e Medidas de Adaptação Projecto SIAM II, Gradiva, Lisboa, 169-208.

Antunes, C. and Taborda, R. (2009). Sea level at Cascais tide gauge: data, analysis and results. Journal of Coastal Research, SI 56 (Proceedings of 10th International Coastal Symposium), 218-222. Lisbon, Portugal, ISBN.

Araújo, I.G.B. (2005). Sea Level Variability: Examples from the Atlantic Coast of Europe. University of Southampton, PhD. Thesis, 411pp.

Araújo, I.G.B., Dias, J.M., Pugh, D.T. (2008). Model simulations of tidal changes in a coastal lagoon, the Ria de Aveiro (Portugal). Continental Shelf Research, 28, 1010-1025.

Bertin, X., Fortunato, A.B., Oliveira, A. (2009). Simulating morphodynamics with unstructured grids: description and validation of a modelling system for coastal applications. Ocean Modelling, 28/1-3, 75-87.

Carter, T.R., Jones, R.N., Lu, X., Bhadwal, S., Conde, C., Mearns, L.O., O'Neill, B.C., Rounsevell, M.D.A., Zurek, M.B. (2007). New Assessment Methods and the Characterisation of Future Conditions. Climate Change 2007: Impacts, Adaptation and Vulnerability. Contribution of Working Group II to the Fourth Assessment Report of the Intergovernmental Panel on Climate Change, M.L. Parry, O.F. Canziani, J.P. Palutikof, P.J. van der Linden, C.E. Hanson, Eds., Cambridge University Press, Cambridge, UK, 133-171.

Chao, B.F., Farr, T., LaBrecque, J., Bindschadler, R., Douglas, B., Rignot, E., Shum, C.K. & Wahr, J. (2002). Understanding Sea Level Change. Available: http://esto.gsfc.nasa.gov/conferences/igarss-2002/02Papers/01061440.

Coelho, C., Silva, R., Veloso-Gomes, F., Taveira-Pinto, F. (2009). Potential effects of climate change on northwest Portuguese coastal zones. ICES Journal of Marine Science, 66, 000-000.

Cunha, L.V., Ribeiro, L., Oliveira, R.P., Nascimento, J. (2006). Recursos Hídricos. Alterações Climáticas em Portugal Cenários, Impactos e Medidas de Adaptação Projecto SIAM II, Gradiva, Lisboa, 115-168.

Dias, J.A. and Taborda, R. (1988). Evolução recente do nível médio do mar em Portugal. Anais do instituto Hidrográfico, 9, 83-97.

Dias, J.M.A., Ferreira, Ó.M.F.C., Pereira, A.P.R.R. (1994). Estudo Sintético da Geomorfologia e da Dinâmica Sedimentar dos Troços Costeiros entre Espinho e a Nazaré. Estudos de Ambiente e Informática, Lda, 261pp.

Dias, J. M., Lopes, J. F., Dekeyser, I. (1999). Hidrological characterization of Ria de Aveiro, Portugal, in early summer. Oceanologica Acta, 22 (5), 473-485.

Dias, J.M., Lopes, J.F., Dekeyser, I. (2000). Tidal propagation in Ria de Aveiro Lagoon, Portugal. Phys. Chem. Earth (B), Vol.25, No. 4, 369-374.

Dias, J.M. (2001). Contribution to the study of the Ria de Aveiro hydrodynamics. Universidade de Aveiro. PhD. Thesis, 288 pp.

Dias, J.M. and Lopes, J.F. (2006). Implementation and assessment of hydrodynamic, salt and heat transport models: The case of Ria de Aveiro Lagoon. Portugal. Environmental Modelling and Software, 21, 1-15.

Douglas, B.C. (1991). Global sea level rise. Journal of Geophysical research, 96, 6981-6992.

Engelund, F., Hansen, F. (1967). A Monograph of Sediment Transport in Alluvial Channels, *Teknisk Forlag*, Copenhagen, Denmark.

Ferreira, Ó., Dias, J.A., Taborda, R. (2008). Implications of Sea-Level Rise for Continental Portugal. Journal of Coastal Research, 24 (2), 317-324.

Fortunato, A.B. and Oliveira, A. (2004). A modeling system for long-term morphodynamics, Journal of Hydraulic Research, 42(4), 426–434.

Fortunato, A.B. and Oliveira, A. (2007). Improving the stability of a morphodynamic modeling system, Journal of Coastal Research, SI 50, 486–49.

Fortunato, A.B., Bertin, X., Oliveira, A. (2009). Space and time variability of uncertainty in morphodynamic simulations. Coastal Engineering, 56, 886-894.

Freitas, R., Sampaio, L., Rodrigues, A., Quintino, V. (2005). Sea-bottom classification across a shallow water bar channel and near-shore shelf, using single-beam acoustics, Estuarine, Coastal and Shelf Science, 625-632.

Friedlingstein, P., Cox, P., Betts, R., Bopp, L., von Bloh, W., Brovkin, V., Cadule, P., Doney, S., Eby, M., Fung, I., Bala, G., John, J., Jones, C., Joos, F., Kato, T., Kawamiya, M., Knorr, W., Lindsay, K., Matthews, H. D., Raddatz, T., Rayner, P., Reick, C., Roeckner, E., Schnitzler, K.-G., Schnur, R., Strassmann, K., Weaver, A. J., Yoshikawa, C., Zeng, N. (2006). Climate Carbon Cycle Feedback Analysis: Results from the C4MIP Model Intercomparison. J. Climate, 19, 3337–3353.

Gregory, J. M., Church, J. A., Boer, G. J., Dixon, K. W., Flato, G. M., Jackett, D. R., Lowe, J. A., O'Farrell, S. P., Roeckner, E., Russell, G. L., Stouffer, R. J., Winton, M. (2001). Comparison of results from several AOGCMs for global and regional sea-level change 1900-2100. Climate Dynamics, 18, 241-253.

Katsman, A.C., Hazeleger, W., Drijfhout, S.S., Oldenborgh, G.J., Burges, G.J.H. (2007). Climate scenarios of sea level rise for the northeast Atlantic Ocean: a study including the effects of ocean dynamics and gravity changes induced by ice melt. Kluwer Academic Publishers, Netherlands.

Larangeiro, S.H.C.D. and Oliveira, F.S.B.F. (2003). Assessment of the longshore sediment transport at Buarcos beach (West Coast of Portugal) through different formulations. Proceedings of CoastGis'03 (Genoa, Italy).

Large, W.G., McWilliams, J. C., Doney, S.C. (1994), Oceanic vertical mixing: Review and a model with non-local boundary layer parameterization. Rev. Geophys., 32, 363-403.

Lopes, J.F. and Dias, J.M., (2007). Residual circulation and sediment distribution in the Ria de Aveiro lagoon, Portugal. Journal of Marine Systems, 68, 507-528.

Martins, V., Rodrigues, S., Grangeia, C., Bernardes, C., Silva, P., Dias, J.M, Rocha, F. (2007). Sediments erosion/deposition in the Ria de Aveiro inlet. Book of Abstracts ISMS07, International Symposium in Marine Sciences, Valência, Spain, 28-31 March, p. 142.

Meehl, G., Stocker, T. F., Collins, W. D., Friedlingstein, P., Gaye, A. T., Gregory, J. M., Kitoh, A., Knutti, R., Murphy, J. M., Noda, A., Raper, S. C. B., Watterson, I. G., Weaver, A. J., Zhao, Z.-C. (2007a). Global Climate Projections. In: Solomon, S., Qin, D., Manning, M., Chen, Z., Marquis, M., Averyt, K. B., Tignor, M., Mille, H. L. (eds.). Climate Change 2007: The Physical Science Basis. Contribution of Working Group I to the Fourth Assessment Report of the Intergovernmental Panel on Climate Change. Cambridge University Press, Cambridge, United Kingdom and New York, NY, USA.

Meehl, G. A., Covey, C., Delworth, T., Latif, M., McAvaney, B., Mitchell, J. F. B., Stouffer, R. J., Taylor, K. E. (2007b). The WCRP CMIP3 multi-model dataset: A new era in climate change research, Bulletin of the American Meteorological Society, 88, 1383-1394.

Morgan, M.G. and Henrion, M. (1990). Uncertainty: A Guide to Dealing with Un- certainty in Quantitative Risk and Policy Analysis. Cambridge University Press, New York, 344 pp.

Nicholls, R.J., Wong, P.P., Burkett, V.R., Codignotto, J.O., Hay, J.E., McLean, R.F., Ragoonaden, S., Woodroffe, C.D. (2007). Coastal systems and low-lying areas. Climate Change 2007: Impacts, Adaptation and Vulnerability. Contribution of Working Group II

to the Fourth Assessment Report of the Intergovernmental Panel on Climate Change, Parry, M.L., Canziani, O.F., Palutikof, J.P., van der Linden, P.J., Hanson, C.E. (Eds.), Cambridge University Press, Cambridge, UK, 315-356.

Oliveira, A., Fortunato, A.B., Dias, J.M. (2006). Numerical modeling of the Aveiro inlet dynamics. In: Proc. of the 30th International Conference on Coastal Engineering, Smith, J.M. (Ed.) Vol. 4, pp3282–3294, World Scientific Publishing Co.

Peltier, W. R. (2004). Global Glacial Isostasy and the Surface of the Ice-Age Earth: The ICE-5G (VM2) Model and GRACE, Ann. Rev. Earth and Planet. Sci., 32, 111-149.

Picado, A. (2008). Degradation of the salt pans in Ria de Aveiro: An Hydrodynamical Study. MSc. Thesis, University of Aveiro, Portugal, 50 pp.

Plecha, S., Rodrigues, S., Silva, P., Dias, J.M., Oliveira, A., Fortunato, A.B. (2007). Trends of bathymetric variations at a tidal inlet, Proceedings of the 5th IAHR Symposium on River, Coastal and Estuarine Morphodynamics, Enschede, The Netherlands, Eds M. Dohmen- Janssen & S. Hulscher, pp. 19-23. ISBN: 0415453631.

Plecha, S., Silva, P.A., Vaz, N., Bertín, X., Oliveira, A., Fortunato, A.B., Dias, J.M. (2009). Sensitivity analysis of a morphodynamic modeling system applied to a coastal lagoon inlet. Submitted to Ocean Dynamics.

Russell, G.L., Miller, J.R., Rind D. (1995). A coupled atmosphere-ocean model for transient climate change studies. Atmos.-Ocean, 33, 683-730.

Russell, G.L., Miller, J.R., Rind D., Ruedy, R.A., Schmidt, G.A., Sheth, S. (2000). Comparison of model and observed regional temperature changes during the past 40 years. J. Geophys. Res., 105, 14891--14898.

Silva, J.F. and Duck, R.W. (2001). Historical changes of bottom topography and tidal amplitude in the Ria de Aveiro, Portugal – trends for future evolution. Climate Research, 18, 17-24.

Solomon, S., Qin, D., Manning, M., Alley, R.B., Berntsen, T., Bindoff, N.L., Chen, Z., Chidthaisong, A., Gregory, J.M., Hegerl, G.C., Heimann, M., Hewitson, B., Hoskins, B.J., Joos, F., Jouzel, J., Kattsov, V., Lohmann, U., Matsuno, T., Molina, M., Nicholls, N., Overpeck, J., Raga, G., Ramaswamy, V., Ren, J., Rusticucci, M., Somerville, R., Stocker, T.F., Whetton, P., Wood, R.A., Wratt, D. (2007). Technical Summary. In: Climate Change 2007: The Physical Science Basis. Contribution of Working Group I to the Fourth Assessment Report of the Intergovernmental Panel on Climate Change. Solomon, S., Qin, D., Manning, M., Chen, Z., Marquis, M., Averyt, K.B., Tignor M., Miller, H.L. (eds.), Cambridge University Press, Cambridge, United Kingdom and New York, NY, USA.

Vaz, N. and Dias, J.M. (2008). Hydrographic characterization of an estuarine tidal channel. Journal of Marine Systems, 70, 168-181.

Zang, Y., Baptista, A., Meyers, E. (2004). A cross-scale model for 3D baroclinic circulation in estuary-plume-shelf systems: I. Formulation and skill assessment. Continental Shelf Research, 24, 2187-2214.